Fig. 2

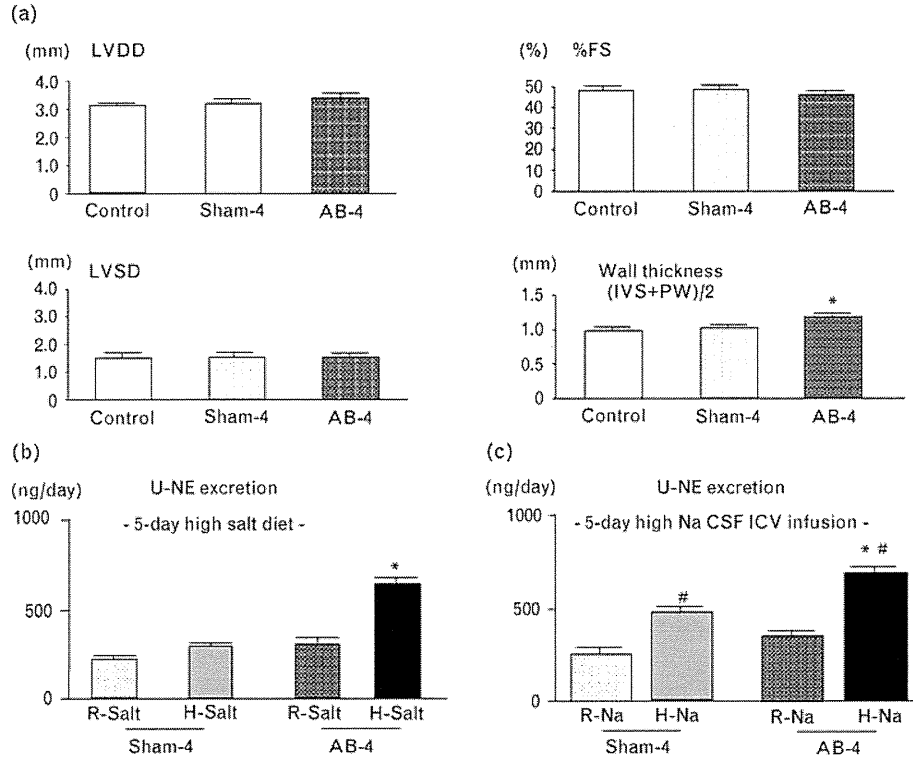

(a) Cardiac function in each group. %FS, percentage fractional shortening; IVS, interventricular septum; LVDD, left-ventricular end-diastolic diameter; LVSD, left-ventricular systolic diameter; PW, posterior wall. $^{*}P < 0.05$ versus other group, $n = 5$ for each. (b) U-NE excretion in response to 5-day high-salt diet in each group. H-salt, high-salt diet; R-salt, regular-salt diet. $^{*}P < 0.05$ versus R-salt, $n = 7$–8. (c) U-NE excretion in response to 5-day ICV infusion of high-Na CSF in each group. H-Na, high-Na CSF; R-Na, regular-Na CSF. $^{\#}P < 0.05$ versus R-Na, $^{*}P < 0.05$ versus Sham-4 H-Na, $n = 7$ for each. CSF, cerebrospinal fluid; ICV, intracerebroventricular; U-NE, urinary norepinephrine.

Statistical analysis

All values are expressed as mean ± SE. Analysis of variance was used to compare U-NE, organ weight, LVDD, LVSD, LVWT, %FS, and protein expression levels between groups. An unpaired *t*-test was used to compare changes in protein levels between AB-H mice treated with and without eplerenone. Differences were considered to be significant when the *P* value was less than 0.05.

Results

Characteristics of AB-4 mice

Neither relative heart weight (heart weight/body weight) nor absolute heart weight differed between AB-4 mice and Sham-4 mice (relative heart weight: Sham-4, 5.08 ± 0.11; AB-4, 5.10 ± 0.10, absolute heart weight: Sham-4, 0.23 ± 0.04 g; AB-4, 0.23 ± 0.06 g, $n = 4$ for each). Relative lung weight (lung weight/body weight) also did not differ between groups (relative lung weight: Sham-4, 5.64 ± 0.21 g; AB-4, 5.90 ± 0.23 g, $n = 4$ for each).

Echocardiography revealed the following characteristics (Fig. 2a): LVWT was greater in AB-4 mice than in Sham-4 mice. The LV dimension and %FS, however, did not differ between groups.

Sympathetic activity evaluated by U-NE excretion in response to the 5-day high-salt diet was increased in AB-4 mice, but not in Sham-4 mice (Fig. 2b). Sympathetic activity in response to a 5-day ICV infusion of high-Na CSF was increased in both Sham-4 mice and AB-4 mice (Fig. 2c). LV systolic function evaluated by echocardiography did not change after the 5-day high-salt diet or after 5-day ICV infusion of high-Na CSF in either AB-4 mice or Sham-4 mice (data not shown).

Mineralocorticoid receptor, epithelial Na channel, and AT1R expression in the circumventricular tissue in AB-4 mice

Mineralocorticoid receptor expression was significantly greater in AB-4 mice than in Sham-4 mice (Fig. 3a). αENaC expression was significantly increased in AB-4 mice compared with Sham-4 mice (Fig. 3b), but βENaC and γENaC expression did not differ between groups (Fig. 3c). AT1R expression was greater in AB-4 mice than in Sham-4 mice (Fig. 3d). The enhanced brain αENaC and AT1R expression was attenuated by ICV infusion of eplerenone (Fig. 3b,d). The enhanced brain mineralocorticoid receptor and αENaC expressions did not

Fig. 3

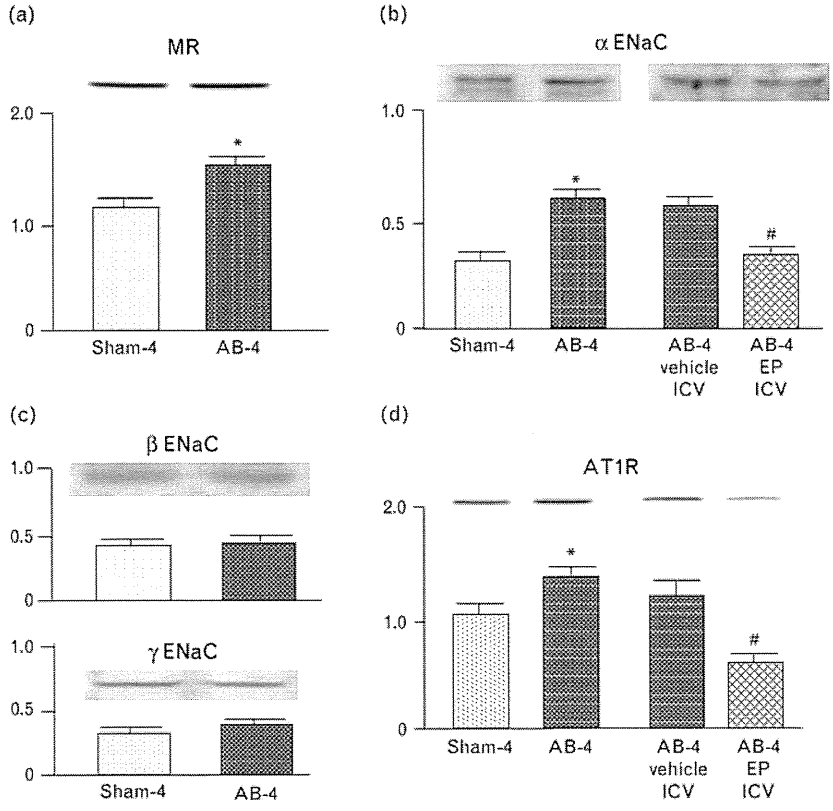

(a–c)Representative western blots showing MR, α, β, and γENaC expression in the brain from each group of mice. The graph shows the means for the quantification of four separate experiments. Data are expressed as the relative ratio to GAPDH expression. $^{*}P<0.05$ versus Sham-4, $^{\#}P<0.05$ versus AB-4 vehicle ICV. (d) Representative western blots showing AT1R expression in the brain. The graphs show the means for the quantification of three separate experiments. Data are expressed as the relative ratio to GAPDH expression. $^{*}P<0.05$ versus Sham-4, $^{\#}P<0.05$ versus AB-4 vehicle ICV. AT1R, angiotensin II type 1 receptor; EP, eplerenone; GAPDH, glyceraldehyde 3-phosphate dehydrogenase; ICV, intracerebroventricular infusion; MR, mineralocorticoid receptor.

change by ICV infusion of telmisartan (relative abundance of mineralocorticoid receptor/GAPDH: 1.76 ± 0.12 in AB-4 with vehicle versus 1.67 ± 0.11 in AB-4 with telmisartan, relative abundance of αENaC/GAPDH: 0.59 ± 0.08 in AB-4 with vehicle versus 0.61 ± 0.09 in AB-4 with telmisartan $n=3$ for each).

Effects of eplerenone on sympathetic activity in response to high-salt diet

Intracerebroventricular infusion of eplerenone started concomitantly with aortic banding attenuated sympathetic activity in response to the 5-day high-salt diet in AB-4 mice (U-NE: AB-4 high-salt diet with eplerenone, 397 ± 40 ng/day; AB-4 high-salt diet without eplerenone, 650 ± 30 ng/day, $n=5$–7).

Effects of long-term high-salt intake on sympathetic activity and left-ventricular systolic function in AB-H mice

Relative heart weight (heart weight/body weight) was significantly increased in AB-H mice compared with Sham mice (Sham-R, 4.81 ± 0.10; Sham-H, 5.11 ± 0.18; AB-R, 5.54 ± 0.20; AB-H, 6.62 ± 0.21, $n=4$ for each). Absolute heart weight was also significantly greater in AB-H mice than in Sham mice (Sham-R, 0.23 ± 0.01 g; Sham-H, 0.24 ± 0.02 g; AB-R, 0.25 ± 0.01 g; AB-H, 0.27 ± 0.02 g, $n=4$ for each). Relative lung weight (lung weight/body weight) did not differ significantly between groups (Sham-R, 5.81 ± 0.21; Sham-H, 5.73 ± 0.14; AB-R, 5.94 ± 0.12; AB-H, 6.24 ± 0.23, $n=4$ for each). Body weight was significantly lower in AB mice than in Sham mice (Sham-R, 47.8 ± 0.5 g; Sham-H, 47.1 ± 0.5; AB-R, 44.2 ± 0.9; AB-H, 40.2 ± 0.4, $n=4$ for each).

Echocardiography revealed the following characteristics (Fig. 4a): LVWT was greater in AB mice than in Sham mice. %FS was significantly lower in AB-R mice than in Sham mice and further decreased in AB-H mice than in AB-R mice. The LV size was significantly higher in AB-H mice than in the other groups. Echocardiography revealed no significant differences between Sham-R mice and Sham-H mice.

Sympathetic activity evaluated by U-NE excretion was significantly higher in AB-H mice than in the other

Fig. 4

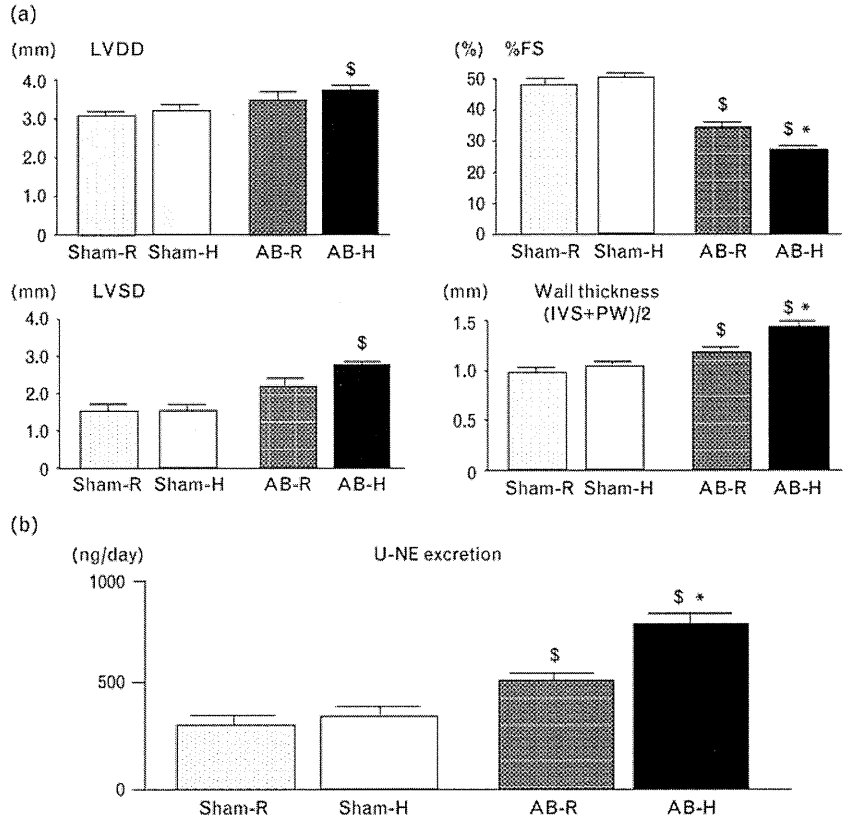

(a) Cardiac function in each group. %FS, percentage fractional shortening; IVS, interventricular septum; LVDD, left-ventricular end-diastolic diameter; LVSD, left-ventricular systolic diameter; PW, posterior wall. $^{\$}P < 0.05$ versus Sham mice (Sham-R and Sham-H), $^{*}P < 0.05$ versus AB-R, $n = 5$ for each. (b) Sympathetic activity evaluated by U-NE excretion in each group. $\$P < 0.05$ versus Sham mice (Sham-R and Sham-H), $^{*}P < 0.05$ versus AB-R, $n = 10$ for each. U-NE, urinary norepinephrine.

groups (Fig. 4b). Blood pressure in AB-H mice tended to be lower, and heart rate was significantly higher than that in the other groups [mean blood pressure (mmHg): 99 ± 5 in Sham-R, 95 ± 2 in Sham-H, 90 ± 3 in AB-R, 82 ± 2 in AB-H, heart rate (b.p.m.): 409 ± 7 in Sham-R, 428 ± 5 in Sham-H, 440 ± 6 in AB-R, 464 ± 8 in AB-H, $n = 5$ for each].

Mineralocorticoid receptor, epithelial Na channel, and AT1R expression in the circumventricular tissue in AB-H mice

Mineralocorticoid receptor expression was significantly greater in AB-H mice than in Sham mice (Fig. 5a). Mineralocorticoid receptor expression in AB-R mice was similar to that in AB-H mice. Mineralocorticoid receptor expression in Sham-H mice did not differ from that in Sham-R mice.

αENaC expression did not differ between groups (Sham-R, Sham-H, AB-R, and AB-H mice; Fig. 5b). γENaC expression, however, was significantly increased in AB-H mice compared with Sham mice. γENaC expression in AB-R mice was similar to that in AB-H mice. γENaC expression in Sham-H mice did not differ from that in Sham-R mice. ICV infusion of eplerenone (administered concomitantly with a high-salt diet) did not attenuate the enhanced γENaC expression (Fig. 5c). βENaC expression did not differ between groups (Fig. 5b). AT1R expression in AB-H was significantly greater than in Sham mice, and ICV infusion of eplerenone attenuated this increase (Fig. 5d).

Effects of eplerenone on left-ventricular systolic function and sympathetic activity in AB-H mice

Intracerebroventricular infusion of eplerenone significantly decreased both relative and absolute heart weight and significantly improved LV systolic function (decreased LVDD and LVSD, increased %FS) in AB-H mice (Fig. 6a). Sympathetic activity was also decreased by ICV infusion of eplerenone in AB-H mice (Fig. 6b). The effects of oral administration of eplerenone were similar to those of ICV infusion. Oral administration of eplerenone had smaller effects on U-NE excretion and %FS than ICV infusion, although oral administration had

Fig. 5

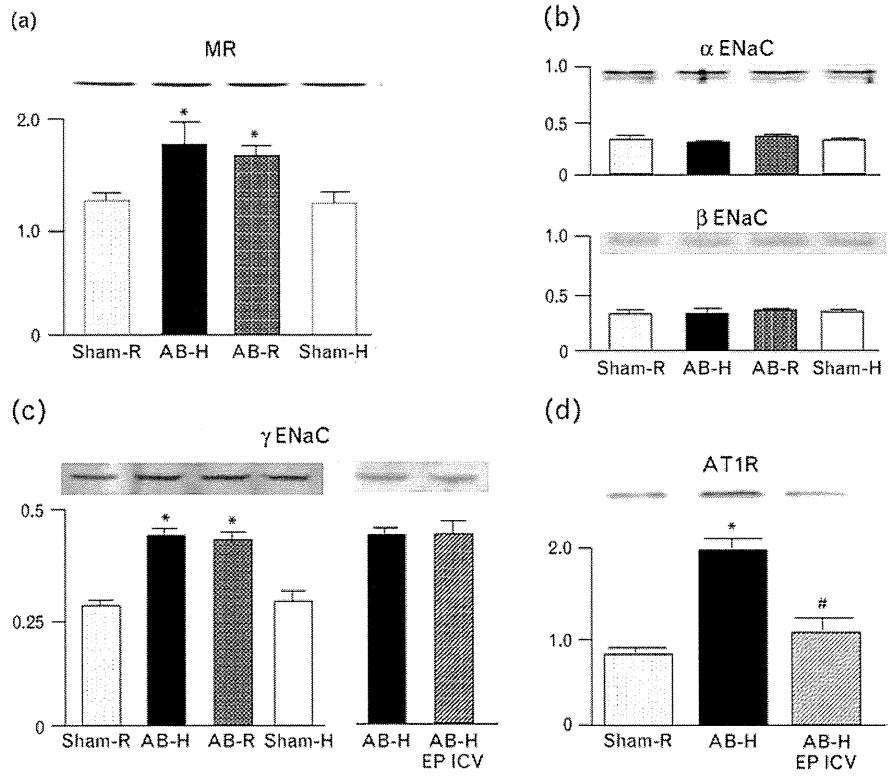

(a) Representative western blots showing MR expression in the brain from each group of mice. The graph shows the means for the quantification of five separate experiments. Data are expressed as the relative ratio to GAPDH expression. $^*P < 0.05$ versus Sham mice (Sham-R and Sham-H). (b-c) Representative western blots showing α, β, and γENaC expression in the brain from each group of mice. The graph shows the means for the quantification of three separate experiments. Data are expressed as the relative ratio to GAPDH expression. $^*P < 0.05$ versus Sham mice (Sham-R and Sham-H). (d) Representative western blots showing AT1R expression in the brainfrom each group of mice. The graph shows the means for the quantification of three separate experiments. Data are expressed as the relative ratio to GAPDH expression. $^*P < 0.05$ versus Sham-R, $^{\#}P < 0.05$ versus AB-H. AT1R, angiotensin II type 1 receptor; EP, eplerenone; GAPDH, glyceraldehyde 3-phosphate dehydrogenase; ICV, intracerebroventricular infusion; MR, mineralocorticoid receptor.

greater effects on LV hypertrophy than ICV infusion (Fig. 6a,b). Neither ICV infusion nor oral administration of eplerenone altered blood pressure [mean blood pressure (mmHg): 82 ± 2 in AB-H versus 88 ± 2 in AB-H with ICV eplerenone, 86 ± 1 in AB-H with oral eplerenone, $n = 5$ for each]. Heart rate, however, was significantly lower in mice treated with either ICV infusion or oral administration of eplerenone [heart rate (b.p.m.): 464 ± 8 in AB-H versus 430 ± 6 in AB-H with ICV eplerenone, 436 ± 12 in AB-H with oral eplerenone, $n = 5$ for each].

Discussion

The present study demonstrated the following: 4 weeks after aortic banding, mice had LV hypertrophy without a decrease in %FS (AB-4 mice); sympathetic activity in response to high salt intake was augmented in AB-4 mice via brain mineralocorticoid receptor-modulated αENaC and AT1R activation; and both ICV infusion and oral administration of eplerenone, a selective mineralocorticoid receptor blocker, attenuated salt-induced sympathetic activation and improved LV systolic function in AB-H mice. These findings indicate that mineralocorticoid receptor antagonism may be a useful strategy to prevent sympathetic activation in response to high salt intake in patients with pressure overload, such as hypertensive heart disease. Furthermore, these effects of mineralocorticoid receptor antagonism may improve LV systolic function by attenuating salt-induced sympathetic activation.

The enhanced brain mineralocorticoid receptor, αENaC, and AT1R expression in AB-4 mice is an important finding in the present study. Brain mineralocorticoid receptor, ENaCs, and AT1R are involved in sympathetic activation in a salt-sensitive hypertensive model [15], a model of high-Na CSF induced hypertension [4], and a myocardial infarction model [16]. Using a mineralocorticoid receptor antagonist in the present study, we confirmed these previous observations. These previous studies, however, did not evaluate whether the expression of these proteins was increased. Therefore, we investigated brain mineralocorticoid receptor, ENaC, and AT1R expression and

Fig. 6

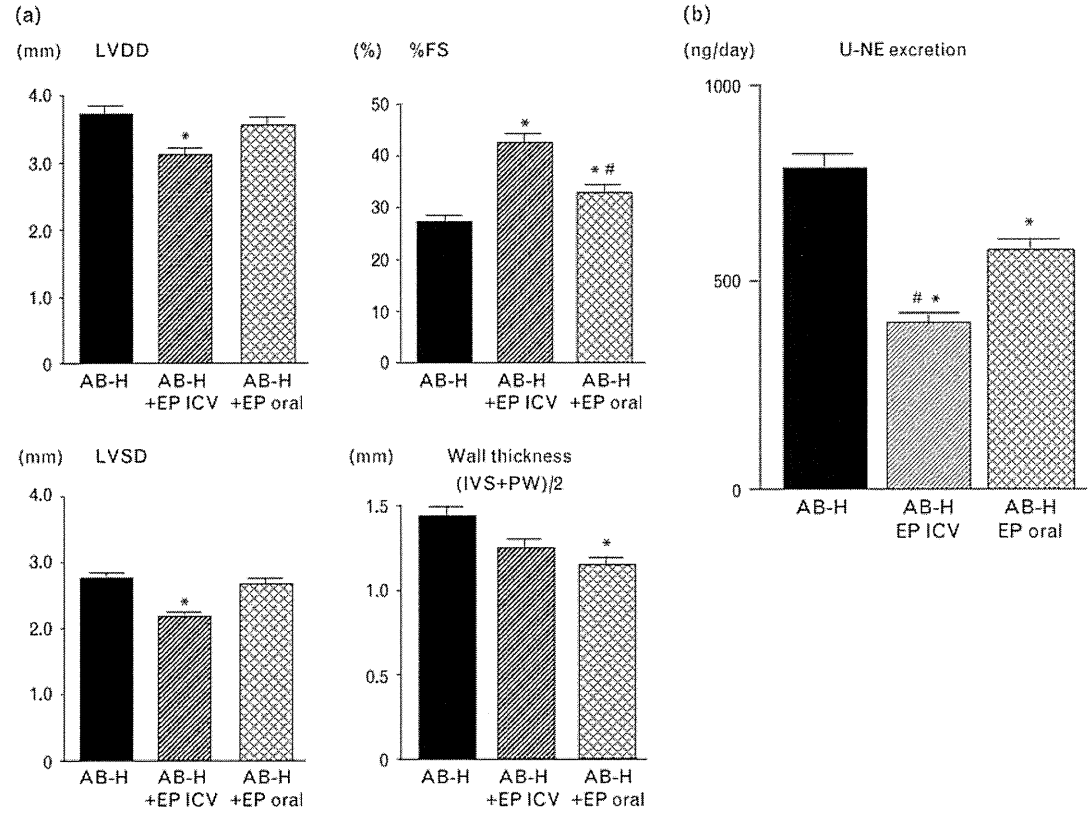

(a) Cardiac function in each group. EP, eplerenone; %FS, percentage fractional shortening; ICV, intracerebroventricular infusion, IVS, interventricular septum; LVDD, left-ventricular end-diastolic diameter; LVSD, left-ventricular systolic diameter; PW, posterior wall. $^{*}P < 0.05$ versus AB-H, $^{\#}P < 0.05$ versus AB-H EP ICV, $n = 5$ each. (b) Sympathetic activity evaluated by U-NE excretion in each group. EP, eplerenone; ICV, intracerebroventricular infusion. $^{*}P < 0.05$ versus AB-H mice, $^{\#}P < 0.05$ versus AB-H EP ICV mice, $n = 6$ in AB-H EP ICV and EP oral, $n = 10$ in AB-H.

confirmed the enhanced expression of these proteins in AB-4 mice. Furthermore, we confirmed that ICV infusion of eplerenone attenuated the enhanced brain αENaC and AT1R expression, but ICV infusion of telmisartan failed to attenuate the enhanced expression of brain mineralocorticoid receptor and αENaC. These results strongly suggest that, in AB-4 mice, activation of the brain MR-αENaC pathway leads to AT1R activation. This brain mineralocorticoid receptor–αENaC pathway activation may facilitate Na uptake from plasma to the CSF, because ENaCs on the blood side of the choroidal epithelium have an important role in Na transport into the CSF [5,6]. Therefore, activation of the brain mineralocorticoid receptor–αENaC pathway is considered to be an initial step in the acquisition of Na sensitivity in the brain in a pressure overload model.

We confirmed the important role of the brain mineralocorticoid receptor–αENaC pathway in the acquisition of Na sensitivity in a pressure overload model. Sympathetic activity in response to the 5-day high-salt diet was increased in AB-4 mice, but not in Sham-4 mice. On the contrary, sympathetic activity in response to ICV infusion of high-Na CSF was increased in both Sham-4 mice and AB-4 mice. These results support the notion that enhanced Na uptake into the CSF is an important factor in salt-induced sympathetic activation in a pressure overload model. Furthermore, the 5-day high-salt diet-induced sympathetic activation in AB-4 mice was attenuated by ICV infusion of eplerenone started concomitantly with aortic banding. These results indicate that the brain mineralocorticoid receptor–αENaC pathway has an important role in the acquisition of Na sensitivity in the brain in a pressure overload model. Although U-NE was increased by ICV infusion of high-Na CSF in both AB-4 mice and Sham-4 mice, the extent of the increase was greater in AB-4 mice than in Sham-4 mice, suggesting that sensitivity to Na in the CSF was increased in AB-4 mice. These findings support those in our previous study [9], but the underlying mechanism remains unclear. In addition to the mineralocorticoid receptor-modulated increase in αENaC expression in the brain, in the present study we confirmed that mineralocorticoid receptor also modulates the expression of AT1R in the brain.

Therefore, enhanced AT1R expression might contribute to the increased responsiveness to Na in the CSF in AB-4 mice.

To clarify the effects of long-term high-salt diet on sympathetic activity and LV systolic function in a pressure overload model, we fed AB-4 mice and Sham-4 mice a high-salt or regular-salt diet for 4 weeks. U-NE excretion increased in AB-R mice compared with Sham mice, and further increased in AB-H mice compared with AB-R mice. LVWT increased and %FS decreased in AB-R mice compared with Sham mice, and both alterations were more severe in AB-H mice than in AB-R mice. U-NE excretion and LVWT, and %FS did not differ between Sham-H mice and Sham-R mice. Blood pressure was lower and heart rate was higher in AB-H mice than in the other groups, suggesting low cardiac output and sympathetic activation [9]. These results strongly suggest that, in a pressure-overload model, long-term high-salt intake accelerates sympathetic activation, resulting in the deterioration of LV systolic function.

Another important finding of the present study was that the enhanced brain mineralocorticoid receptor expression in the pressure-overload model was maintained in AB-H mice, and treatment with eplerenone reduced salt-induced sympathetic activation and LV systolic dysfunction in the AB-H mice. These results indicate that activation of the brain mineralocorticoid receptor pathway is sustained under high-salt loading in AB-H mice. Because serum aldosterone levels are significantly decreased in this model [9], activation of the brain mineralocorticoid receptor in AB-H mice might be independent of systemic aldosterone levels. CSF-Na may increase the local production of aldosterone in the brain [15,17], or there may be aldosterone-independent mineralocorticoid receptor activation [18]. The present study, however, did not address these issues, and further studies are needed to clarify the mechanisms of the enhanced expression of brain mineralocorticoid receptor in AB mice.

Both ICV infusion and oral administration of eplerenone for 4 weeks concomitantly with high-salt loading in AB-H mice attenuated the salt-induced sympathetic activation and improved LV systolic dysfunction. Because CSF eplerenone concentrations were not measured in the present study we cannot determine the concentration of eplerenone in the brain required to induce these observations via central mechanisms. In the present study, oral administration of eplerenone attenuated LV hypertrophy, which might be a direct effect of oral administration of eplerenone on the myocardium [10,11]. Blood pressure is another factor involved in LV hypertrophy. In the present study, neither oral administration nor ICV infusion of eplerenone affected blood pressure in AB-H mice. Blood pressure was measured under anesthesia, however, and we did not evaluate the 24-h blood pressure. Therefore, we cannot exclude the possibility that blood pressure affected LV hypertrophy. Heart rate was significantly decreased in AB-H with eplerenone, suggesting that sympathetic activity was attenuated. The dose of eplerenone was based on the maximum water solubility of eplerenone in an ICV infusion study, and by the most commonly used dose of eplerenone as a specific mineralocorticoid receptor blocker in oral administration studies [19,20,21]. In a previous study, eplerenone was injected into the hypothalamus at a dose of 0.13 mg/ml, 18 μl/h [22]. In the present study, we performed ICV infusion. In ICR mice, the CSF volume is approximately 36 μl [23]. Therefore, the dose of ICV-infused eplerenone in the present study was a relatively small dose (0.3 mg/ml, 0.11 μl/h) that should have produced an end concentration that acts as a specific mineralocorticoid receptor antagonist.

To explore the mechanisms of the inhibitory effects of eplerenone on salt-induced sympathetic activation and LV systolic dysfunction, we focused on the mineralocorticoid receptor–ENaC pathway. First, we examined the brain ENaC expression in both high-salt and regular-salt Sham mice and AB mice. Unlike in the AB-4 mice, the expression of αENaC did not differ between groups. The expression of γENaC, however, was significantly greater in AB-R mice than in Sham mice. Furthermore, this enhanced expression of γENaC was also evident in AB-H mice. Because of the enhanced brain γENaC expression in AB-H mice, we investigated the effects of ICV infusion of eplerenone on brain γENaC expression. The expression of γENaC was not decreased by ICV infusion of eplerenone. This finding suggests that the enhanced brain γENaC expression is independent of mineralocorticoid receptor activation. Therefore, we examined the involvement of the brain mineralocorticoid receptor–AT1R pathway in the salt-induced sympathetic activation in AB-H mice because we previously confirmed that ICV infusion of an AT1R blocker attenuated the salt-induced sympathetic activation in AB-H mice because we previously confirmed that ICV infusion of an AT1R blocker attenuated the salt-induced sympathetic activation in AB-H mice [9], and also mineralocorticoid receptor blockade attenuates the renin–angiotensin system [24]. The expression of AT1R in the brain was significantly higher in AB-H mice than in Sham mice, and this enhanced expression of AT1R was attenuated by ICV infusion of eplerenone. The brain renin–angiotensin system is activated in a heart failure model [25,26] and contributes to sympathetic hyperactivation [27,28]. These results suggest that the inhibitory effects of eplerenone on salt-induced sympathetic activation and LV systolic dysfunction result from the suppression of AT1R activity.

We evaluated three ENaC subunits, αENaC, βENaC, and γENaC [29]. We demonstrated mineralocorticoid receptor-dependent αENaC enhancement in AB-4 mice,

and mineralocorticoid receptor-independent γENaC enhancement in AB-R mice and AB-H mice. The amount of βENaC did not differ between groups. Although it is generally accepted that ENaC activation occurs through mineralocorticoid receptor activation [7,8], mineralocorticoid receptor-independent ENaC activation has been reported [30]. The mechanisms of mineralocorticoid receptor-independent γENaC activation, however, are unknown. We did not measure Na concentration in the CSF in the present study because of technical difficulties, and we did not directly evaluate the effects of ENaC activity on Na transport. Furthermore, ENaC expression levels may reflect both epithelial components and neural components [6]. We did not address these issues in the present study, and further studies are needed.

In conclusion, the present findings strongly suggest that activation of brain αENaC and AT1R through mineralocorticoid receptor contributes to the acquisition of Na sensitivity to induce sympathoexcitation. High salt intake accelerates sympathetic activation and LV systolic dysfunction in a pressure overload model.

Acknowledgements

We express our sincere thanks to Naomi Shirouzu for help with the western blot analysis.

Sources of funding: This work was supported by Grants-in-Aid for Scientific Research from the Japan Society for the Promotion of Science (B19390231, 19890148, 21790730) and the Mitsubishi Pharma Research Foundation.

There are no conflicts of interest.

References

1 Huang BS, Amin MS, Leenen FHH. The central role of the brain in salt-sensitive hypertension. *Curr Opin Cardiol* 2006; **21**:295–304.
2 Fujita M, Ando K, Nagae A, Fujita T. Sympathoexcitation by oxidative stress in the brain mediates arterial pressure elevation in salt-sensitive hypertension. *Hypertension* 2007; **50**:360–367.
3 Huang BS, Van Vliet BN, Leenen FHH. Increases in CSF [Na+] precede the increases in blood pressure in Dahl S rats and SHR on high-salt diet. *Am J Physiol Heart Circ Physiol* 2004; **287**:H1160–H1166.
4 Huang BS, Cheung WJ, Wang H, Tan J, White RA, Leenen FHH. Activation of brain renin-angiotensin-aldosterone system by central sodium in Wistar rats. *Am J Physiol Heart Circ Physiol* 2006; **291**:H1109–H1117.
5 Vigne P, Champigny G, Marsaut R, Barbry P, Frelin C, Lazdunski M. A new type of amiloride-sensitive cation channel in endothelial cells of brain microvessels. *J Biol Chem* 1989; **264**:7663–7668.
6 Amin MS, Wang HW, Reza E, Whitman SC, Tuana BS, Leenen FHH. Distribution of epithelial sodium channels and mineralocorticoid receptors in cardiovascular regulatory centers in rat brain. *Am J Physiol Regul Integr Comp Physiol* 2005; **289**:R1787–R1797.
7 Muller OG, Parnova RG, Centeno G, Rossier BC, Firsov D, Horisberger JD. Mineralocorticoid effects in the kidney: correlation between (ENaC, GILZ, and Sgk-1 mRNA expression and urinary excretion of Na+ and K+. *J Am Soc Nephrol* 2003; **14**:1107–1115.
8 Pearce D, Kleyman TR. Salt, sodium channels, and SGK1. *J Clin Invest* 2007; **117**:592–595.
9 Ito K, Hirooka Y, Sunagawa K. Acquisition of brain Na sensitivity contributes to salt-induced sympathoexcitation and cardiac dysfunction in mice with pressure overload. *Circ Res* 2009; **104**:1004–1011.
10 Brown NJ. Eplerenone cardiovascular protection. *Circulation* 2003; **107**:2512–2518.
11 Davis KL, Nappi JM. The cardiovascular effects of eplerenone, a selective aldosterone-receptor antagonist. *Clin Ther* 2003; **25**:2647–2668.
12 Harada K, Komuro I, Shiojima I, Hayashi D, Kudoh S, Mizuno T, *et al.* Pressure overload induces cardiac hypertrophy in angiotensin II type II 1A receptor knockout mice. *Circulation* 1998; **97**:1952–1959.
13 Sakai K, Hirooka Y, Shigematsu H, Kishi T, Ito K, Shimokawa H, *et al.* Overexpression of eNOS in brain stem reduces enhanced sympathetic drive in mice with myocardial infraction. *Am J Physiol Heart Circ Physiol* 2005; **289**:H2159–H2166.
14 Ito K, Kimura Y, Hirooka Y, Sagara Y, Sunagawa K. Activation of Rho-kinase in the brainstem enhances sympathetic drive in mice with heart failure. *Auton Neurosci* 2008; **142**:77–81.
15 Huang BS, White RA, Jeng AY, Leenen FHH. Role of CNS aldosterone synthase and mineralocorticoid receptors in salt-induced hypertension in Dahl salt-sensitive rats. *Am J Physiol Regul Integr Comp Physiol* 2009; **296**:R994–R1000.
16 Huang BS, Leenen FHH. Blockade of brain mineralocorticoid receptors or Na+ channels prevents sympathetic hyperactivity and improves cardiac function in rats post-MI. *Am J Physiol Heart Circ Physiol* 2005; **288**:H2491–H2497.
17 Taira M, Toba H, Murakami M, Iga I, Serizawa R, Murata S, *et al.* Spironolactone exhibits direct renoprotective effects and inhibits renal renin-angiotensin-aldosterone system in diabetic rats. *Eur J Pharmacol* 2008; **589**:264–271.
18 Shibata S, Nagase M, Yoshida S, Kawarazaki W, Kurihara H, Tanaka H, *et al.* Modification of mineralocorticoid receptor function by Rac 1 GTPase: implication in proteinuric kidney disease. *Nat Med* 2008; **14**:1370–1376.
19 Nagata K, Obata K, Xu J, Ichihara S, Noda A, Kimata H, *et al.* Mineralocorticoid receptor antagonism attenuates cardiac hypertrophy and failure in low-aldosterone hypertensive rats. *Hypertension* 2006; **47**:656–664.
20 Enomoto S, Yoshiyama M, Omura T, Matsumoto R, Kusuyama T, Kim S, *et al.* Effects of eplerenone on transcriptional factors and mRNA expression related to cardiac remodeling after myocardial infarction. *Heart* 2005; **91**:1595–1600.
21 Sartório CL, Fraccarollo D, Galuppo P, Leutke M, Ertl G, Stefanon I, *et al.* Mineralocorticoid receptor blockade improves vasomotor dysfunction and vascular oxidative stress early after myocardial infarction. *Hypertension* 2007; **50**:919–925.
22 Gabor A, Leenen FHH. Mechanisms in the PVN mediating local and central sodium-induced hypertension in Wistar rats. *Am J Physiol Regul Integr Comp Physiol* 2009; **296**:R618–R630.
23 Rudick RA, Zirretta DK, Herndon RM. Clearance of albumin from mouse subarachnoid space: a measure of CSF bulk flow. *J Neurosci Methods* 1982; **6**:253–259.
24 Zhu A, Yoneda T, Demura M, Karashima S, Usukura M, Yamagishi M, *et al.* Effects of mineralocorticoid receptor blockade on renal renin-angiotensin system in Dahl salt-sensitive hypertensive rats. *J Hypertens* 2009; **27**:800–805.
25 Zhang ZH, Francis J, Weiss RM, Felder RB. The renin-angiotensin-aldosterone system excites hypothalamic paraventricular nucleus neurons in heart failure. *Am J Physiol Heart Circ Physiol* 2002; **283**:H423–H433.
26 Zhu GQ, Gao L, Patel KP, Zucker IH, Wang W. ANG II in the paraventricular nucleus potentiates the cardiac sympathetic afferent reflex in rats with heart failure. *J Appl Physiol* 2004; **97**:1746–1754.
27 Shigematsu H, Hirooka Y, Eshima K, Shihara M, Tagawa T, Takeshita A. Endogenous angiotensin II in the NTS contributes to sympathetic activation in rate with aortocaval shunt. *Am J Physiol Regul Integr Comp Physiol* 2001; **280**:R1665–R1673.
28 Sagara Y, Hirooka Y, Nozoe M, Ito K, Kimura Y, Sunagawa K. Pressor response induced by central angiotensin II is mediated by activation of Rho/Rho-kinase pathway via AT1 receptors. *J Hypertens* 2007; **25**:399–406.
29 Cannessa CM, Schild L, Buell G, Thorens B, Gautschi I, Horisberger JD, *et al.* Amiloride-sensitive epithelial Na+ channel is made of three homologous subunits. *Nature* 1993; **367**:463–467.
30 Nielsen J, Kwon TH, Frokiaer J, Knepper MA, Nielsen S. Maintained ENaC trafficking in aldosterone-infused rats during mineralocorticoid and glucocorticoid receptor blockade. *Am J Physiol* 2007; **292**:F382–F394.

Nanoparticle-mediated endothelial cell-selective delivery of pitavastatin induces functional collateral arteries (therapeutic arteriogenesis) in a rabbit model of chronic hind limb ischemia

Shinichiro Oda, MD,[a] Ryoji Nagahama, MSc,[b] Kaku Nakano, PhD,[b] Tetsuya Matoba, MD,[b] Mitsuki Kubo, MD, PhD,[b] Kenji Sunagawa, MD, PhD,[b] Ryuji Tominaga, MD, PhD,[a] and Kensuke Egashira, MD, PhD,[b] *Fukuoka, Japan*

Objectives: We recently demonstrated in a murine model that nanoparticle-mediated delivery of pitavastatin into vascular endothelial cells effectively increased therapeutic neovascularization. For the development of a clinically applicable approach, further investigations are necessary to assess whether this novel system can induce the development of collateral arteries (arteriogenesis) in a chronic ischemia setting in larger animals.
Methods: Chronic hind limb ischemia was induced in rabbits. They were administered single injections of nanoparticles loaded with pitavastatin (0.05, 0.15, and 0.5 mg/kg) into ischemic muscle.
Results: Treatment with pitavastatin nanoparticles (0.5 mg/kg), but not other nanoparticles, induced angiographically visible arteriogenesis. The effects of intramuscular injections of phosphate-buffered saline, fluorescein isothiocyanate (FITC)-loaded nanoparticles, pitavastatin (0.5 mg/kg), or pitavastatin (0.5 mg/kg) nanoparticles were examined. FITC nanoparticles were detected mainly in endothelial cells of the ischemic muscles for up to 4 weeks. Treatment with pitavastatin nanoparticles, but not other treatments, induced therapeutic arteriogenesis and ameliorated exercise-induced ischemia, suggesting the development of functional collateral arteries. Pretreatment with nanoparticles loaded with vatalanib, a vascular endothelial growth factor receptor (VEGF) tyrosine kinase inhibitor, abrogated the therapeutic effects of pitavastatin nanoparticles. Separate experiments with mice deficient for VEGF receptor tyrosine kinase demonstrated a crucial role of VEGF receptor signals in the therapeutic angiogenic effects.
Conclusions: The nanotechnology platform assessed in this study (nanoparticle-mediated endothelial cell-selective delivery of pitavastatin) may be developed as a clinically feasible and promising strategy for therapeutic arteriogenesis in patients. (J Vasc Surg 2010;52:412-20.)

Clinical Relevance: Restoration of tissue perfusion in patients with critical limb ischemia is a major therapeutic goal. Recent clinical trials designed to induce neovascularization by administering exogenous angiogenic growth factors or cells failed to demonstrate a decisive clinical benefit. A controlled drug delivery system for a new approach to therapeutic neovascularization therefore would be more favorable. In the present study, we applied nanoparticle-mediated delivery system and report that endothelial cell-selective delivery of pitavastatin increased the development of collateral arteries and improved exercise-induced ischemia in a rabbit model of chronic hind limb ischemia. This nanotechnology platform is a promising strategy for the treatment of patients with severe organ ischemia and represents a significant advance in therapeutic arteriogenesis over current approaches.

The vascular endothelium is a major target for the pleiotropic (nonlipid-related) vascular protective effects of the 3-hydroxy-3-methylglutaryl-CoA reductase inhibitors (statins).[1] Statins improve endothelial dysfunction[1-3] and exert multiple vascular protective properties, mainly by enhancing the activity of endothelial nitric oxide synthase. Statins increase the angiogenic activity of mature endothelial cells, as well as that of endothelial progenitor cells, and augment neovascularization (arteriogenesis, vasculogenesis, and angiogenesis) in the ischemic hearts and limbs of

From the Department of Cardiovascular Surgery[a] and Cardiovascular Medicine,[b] Graduate School of Medical Sciences, Kyushu University.
Supported by Grants-in-Aid for Scientific Research (19390216, 19650134) from the Ministry of Education, Science, and Culture, Tokyo, by Health Science Research Grants (Research on Translational Research and Nanomedicine) from the Ministry of Health, Labor, and Welfare, Tokyo; and by grants from New Energy and Industrial Technology Development Organization (NEDO), Kawasaki, Japan.
Competition of interest: Dr Egashira holds a patent on the results reported in the present study.

Additional material for this article may be found online at www.jvascsurg.org.
Reprint requests: Kensuke Egashira, MD, PhD, Department of Cardiovascular Medicine, Kyushu University, 3-1-1, Maidashi, Higashi-ku, Fukuoka, Japan (e-mail: egashira@cardiol.med.kyushu-u.ac.jp).
The editors and reviewers of this article have no relevant financial relationships to disclose per the JVS policy that requires reviewers to decline review of any manuscript for which they may have a competition of interest.
0741-5214/$36.00

doi:10.1016/j.jvs.2010.03.020

experimental animals.[4-6] Statins also attenuate atherosclerosis formation[7] and pose little potential risk for tumor angiogenesis, in contrast to angiogenic growth factors.[8]

Most of these beneficial effects of statins on therapeutic neovascularization, however, were observed after the daily administration of high doses in experimental animals, a regimen that could lead to serious adverse side effects in a clinical setting. A clinical study of 500 patients with coronary artery disease reported no effects of statins within the clinical dose range on indices of functional collateral development (arteriogenesis).[9]

To optimize the therapeutic effects of statins in the induction of therapeutic neovascularization, we recently applied nanotechnology and reported that nanoparticle (NP)-mediated pitavastatin delivery into vascular endothelial cells effectively increased therapeutic neovascularization with no serious side effects in a murine model of acute hind limb ischemia.[10] The beneficial effects induced by pitavastatin-NP were mediated by increased activity of endothelial nitric oxide synthase (eNOS) and multiple endogenous angiogenic growth factors, suggesting that this NP-mediated cell-selective delivery produces a well-harmonized integrative system for therapeutic neovascularization. Importantly, this NP-mediated delivery system was as effective at a dose that is approximately 100 to 300 times lower than the cumulative systemic dose. To translate our experimental findings in the murine model of acute hind limb ischemia to clinically applicable approaches, it is desirable to determine whether NP-mediated statin delivery into vascular endothelial cells induces the development of collateral arteries (arteriogenesis) and thus restores tissue perfusion in a setting of chronic ischemia in larger animals.

Recent evidence suggests that arteriogenesis is a very important adaptive mechanism for the restoration of perfusion to critically ischemic tissue.[11] Arteriogenesis is the process whereby a preexisting arteriole from the resistance vessel class matures into an artery of the conductance vessel class, whereas angiogenesis is the process by which a sprouting capillary originates from a preexisting capillary. Vasculogenesis represents the differentiation of bone marrow-derived endothelial progenitor cells to form a primitive vasculature. The structure and molecular interactions of arteriogenesis differ from those of angiogenesis and vasculogenesis.

Contrary to conventional paradigms,[12] angiogenesis and vasculogenesis by themselves cannot replace the conductance capacity of collateral arteries in the absence of arteriogenesis.[11,13] According to the results of clinical trials, the question has been raised about whether the angiogenesis/vasculogenesis induced by single angiogenic growth factors can induce functional collateral arteries.[14,15] A high local concentration of angiogenic growth factors increases the risk of atherosclerosis[16-18] and tumor angiogenesis.[19] Therefore, an attempt to stimulate the development of functional collateral arteries through the process of arteriogenesis represents an evolution toward a new therapeutic strategy for patients with severe ischemia due to atherosclerotic vascular disease.

The primary aim of this study was to test the hypothesis that NP-mediated delivery of pitavastatin to endothelial cells can be a realistic strategy for promoting functional collateral arteries and for improving exercise-induced ischemia in a rabbit model of chronic hind limb ischemia.

MATERIALS AND METHODS

The study protocol was reviewed and approved by the Committee on Ethics in Animal Experiments, Kyushu University Faculty of Medicine. The experiments were conducted according to the Guidelines of the American Physiological Society.

Preparation of NP. Anionic poly(lactic-co-glycolic acid) (PLGA) NP incorporated with fluorescein-isothiocyanate (FITC), pitavastatin, or vatalanib[20] (an inhibitor of receptor tyrosine kinase of vascular endothelial cell growth factor [VEGF] receptors 1-3; a gift of Novartis Pharma) were prepared by a emulsion solvent diffusion method.[10] The FITC-, pitavastatin-, and vatalanib-incorporated NP contained (w/v) 5% FITC, 6.3% pitavastatin, and 6.1% vatalanib, respectively. The diameter of PLGA NP was 196 ± 29 nm. Additional details are provided in the Appendix (online only).

Angiogenesis activity of human endothelial cells. Angiogenesis of human endothelial cells (HECs) was tested by 2-dimensional Matrigel assay, as previously described.[10] Additional details are provided in the Appendix (online only).

Rabbit model of chronic hind limb ischemia and treatments. Male Japanese White rabbits were used. To induce chronic hind limb ischemia, the left femoral artery was completely excised from its proximal origin at the branchpoint of the external iliac artery to the bifurcation of the saphenous and popliteal arteries.[21,22] For intramuscular injection, drugs incorporated with or without NP were suspended in 5 mL of phosphate-buffered saline (PBS) and injected into 10 different sites in the left medial thigh muscles with a 27-gauge needle 7 days after femoral artery excision (Appendix Fig I, online only). To define the dose-response relationship of the proarteriogenic effects of pitavastatin-NP, animals were randomly divided into a PBS group and three other treatment groups that received an intramuscular injection of pitavastatin-NP containing the three different doses of pitavastatin (0.05, 0.15, and 0.5 mg/kg).

In another set of experiments, animals were randomly distributed in groups receiving intramuscular injections of PBS, pitavastatin (0.5 mg/kg), FITC-NP, or pitavastatin (0.5 mg/kg)-NP. The effect of vatalanib-NP on arteriogenesis induced by pitavastatin-NP was also examined in another set of animals treated intramuscularly with vatalanib-NP or with vatalanib-NP and pitavastatin-NP. Additional details are provided in the Appendix (on-line only).

Effects of pitavastatin-NP on collateral arterial development 28 days after treatment

Internal iliac angiography. A 4Fr end-hole infusion catheter was introduced into the right common carotid

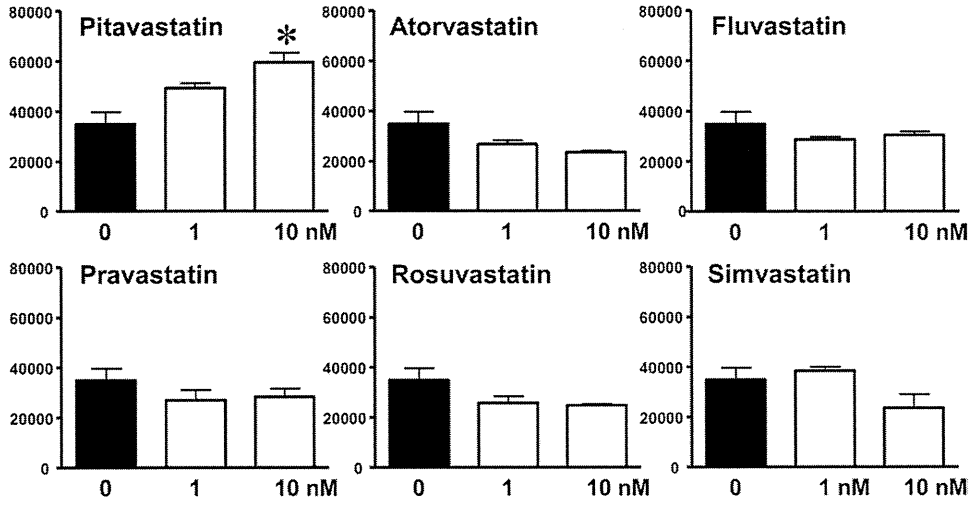

Fig 1. Effects of six statins on angiogenic capacity of human endothelial cells in vitro is shown by quantitative analysis of tube formation (tube length in mm per well) in six independent experiments. $*P < .01$ vs control by one-way analysis of variance with the Dunnett multiple comparison test.

artery and advanced to the left internal iliac artery at the level of the interspaces between the seventh lumbar and the first sacral vertebrae. After an intra-arterial injection of nitroglycerin (0.25 mg), 5 mL of contrast medium was injected at a rate of 1 mL/s. The 3-second angiogram was used for analysis of the angiographic score. A composite of 5-mm^2 grids was placed over the angiogram. The total number of grids that were crossed by visible arteries was divided by the total number of grids in the area of the medial thigh, as previously described.[21,22]

Capillary and arteriolar density. Histologic evaluation was performed for 5-μm frozen sections or 5-μm paraffin-embedded sections of the adductor skeletal muscles of the ischemic limb. $CD31^+$ (Dako, Tokyo, Japan) capillary endothelial cells were counted. Arterioles were determined by immunostaining with α-smooth muscle actin (α-SMA; Dako) and anti-mouse immunoglobulin G secondary antibody (Alexa 546; Molecular Probes, Invitrogen, Carlsbad, Calif), and vessels surrounded by smooth muscle cells were counted. Nuclei were counterstained with 4′,6-diamidino-2-phenylindole (Vector Shield, Vector Laboratories, Burlingame, Calif). Capillary and arteriolar density were calculated as capillaries/mm^2 and arterioles/mm^2 averaged from five randomly selected fields.[21,22] To ensure that the density was not overestimated or underestimated as a consequence of myocyte atrophy or edema, the capillary/muscle and arteriolar/muscle fiber ratios were also evaluated.

Tissue oximetry. Tissue oxygen content was measured by fluorescence quenching technique using an OxyLab PO_2 monitor (Oxford Optronix Ltd, Oxfordshire, UK) fiberoptic probe mounted to a micromanipulator, as previously described.[23] Ischemic limb was exposed on an anesthetized animal, and a 18-gauge needle was used to insert the fiberoptic probe to the adductor skeletal muscles of the ischemic limb at a 90° angle to contact the adductor skeletal muscles. The stable Po_2 reading, before a rapid rise to at least 60 mm Hg that signaled loss of tissue contact, was used as the tissue oxygen partial pressure.

Effects of pitavastatin-NP on forced ischemia induced by electrical pulses. The functional status of collateral arterial development was examined 28 days after treatment with PBS, FITC-NP, pitavastatin only, and pitavastatin-NP. After anesthesia, 21-gauge catheters were inserted into the right femoral artery and the left femoral vein for blood sampling. Two 21-gauge needles were inserted into the left medial thigh and the left gastrocnemius muscle. The electrode wires were then connected to the needles and plugged into the stimulator (Electronic Stimulator, Model SEN-7203, NIHON KOHDEN, Tokyo, Japan). The stimulating voltage was set at 5 V for 1 millisecond to cause noticeable contraction of the left hind limb. The stimulation frequency was 3 Hz, and the left hind limb was electrically stimulated for 30 minutes. Arterial and venous blood was sampled to measure the oxygen saturation before stimulation and at 15 and 30 minutes after stimulation.

A mouse model of hind limb ischemia and treatments. Male wild-type and Flt-1 tyrosine kinase deficient (Flt-1 $TK^{-/-}$) mice[24] were used. After anesthesia, unilateral hind limb ischemia was induced in the mice as previously described.[10,25] Additional details are provided in the Appendix (online only).

Statistical analyses. Data are expressed as mean ± standard error of the mean. Statistical analysis was assessed by one-way or two-way analysis of variance with post hoc test. Values of $P < .05$ were considered statistically significant.

RESULTS

Effects of statins and pitavastatin-NP on the angiogenic capacity of HECs in vitro. Treatment with pitavastatin increased angiogenic activity in HECs, whereas other statins had no effect (Fig 1). Treatment with pitavastatin-

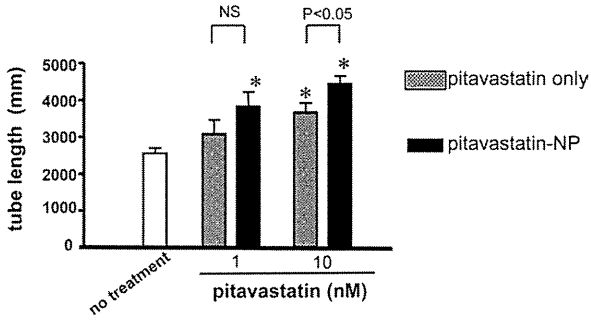

Fig 2. Effects of pitavastatin and pitavastatin nanoparticles *(NP)* are shown on the angiogenic capacity of human endothelial cells in vitro by quantitative analysis of tube formation (tube length per well) of six independent experiments. $*P < .01$ vs control by two-way analysis of variance with the Dunnett multiple comparison test.

NP increased angiogenic activity in HECs. The angiogenic activity of statin-NP was greater than that of 10 nM pitavastatin alone (Fig 2).

Effects of pitavastatin-NP on angiographically visible collateral arterial development. Because only a single dose of pitavastatin (0.4 mg/kg)-NP was previously examined in the mouse model,[13] the dose-response relationship of pitavastatin-NP with angiographically visible collateral arterial development (arteriogenesis) was examined in the present study. Treatment with pitavastatin (0.5 mg/kg)-NP, but not with those with pitavastatin at 0.05 or 0.15 mg/kg, increased the arteriogenic response, as assessed by the angiographic score (Fig 3, *A*). Representative angiograms 28 days after treatment demonstrate corkscrew-like collateral arterial development only in the pitavastatin-NP group (Fig 3, *B*). Treatment with pitavastatin (0.5 mg/kg)-NP significantly increased the angiographic score (Fig 3, *C*). In contrast, no treatment effects on the angiographic score were noted in the FITC-NP or pitavastatin-only groups.

Effects of pitavastatin-NP on histopathologic angiogenesis and arteriogenesis. Treatment with pitavastatin (0.5 mg/kg)-NP, but not with FITC-NP or statin only, significantly increased the capillary density and capillary/muscle fiber ratio, which are indices of angiogenesis (Fig 4, *A*). The beneficial effects of pitavastatin-NP were not associated with significant changes in serum biochemical markers (Table). Treatment with pitavastatin-NP also significantly increased the α-SMA$^+$ arteriolar density and arteriole/muscle fiber ratio, which are indices of arteriogenesis (Fig 4, *B*), indicating that pitavastatin-NP treatment induced angiogenesis and arteriogenesis.

Examination of hematoxylin-eosin-stained sections revealed no abnormal histopathologic findings (inflammation and fibrosis) among the four groups (data not shown). There was no significant difference in muscle fiber density among the four groups (PBS groups: 129 ± 8, 145 ± 4/mm^2; FITC-NP groups: 130 ± 3 and 129 ± 6/mm^2).

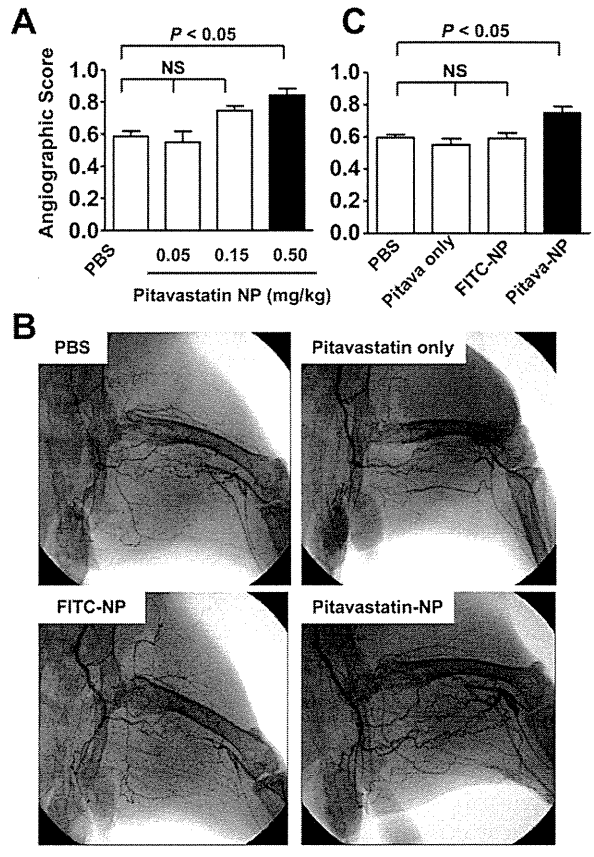

Fig 3. Effects of pitavastatin nanoparticles *(NP)* on angiographically visible collateral arterial development are shown 28 days after treatment. **A,** Effects of pitavastatin-NP containing 0.05, 0.15, or 0.5 mg/kg pitavastatin on the angiographic score (n = 3 each). **B,** Representative angiograms are shown of the phosphate buffered saline *(PBS)*, pitavastatin-only, fluorescein isothiocyanate *(FITC)*-NP, and pitavastatin-NP groups at 28 days after treatment. Corkscrew-like collateral arteries were observed only in the pitavastatin-NP group. **C,** Summary of the angiographic scores obtained for the four groups in panel **B** (n = 6 each).

Effects of pitavastatin-NP on tissue oxygen saturation. The tissue oxygen pressure in adductor skeletal muscles of the ischemic limb was measured 28 days after treatment. Treatment with pitavastatin (0.5 mg/kg)-NP significantly increased tissue oxygen pressure compared with the other groups (Appendix Fig II, online only).

Endothelial cell-selective delivery of NP. The cellular distribution of FITC was examined 3, 7, and 28 days after the intramuscular injection of FITC-NP or FITC only. On day 3 after injection, strong FITC signals were detected in FITC-NP–injected ischemic muscle (Fig 5, *A*), whereas no FITC signals were observed in control nonischemic muscle (Fig 5, *A*) or in ischemic muscle injected with FITC only (data not shown). The FITC signals were localized predominantly to the capillaries and arterioles. Weak FITC signals were also detected in myocytes at day 3t. On day 7 and 28, FITC signals remained localized predomi-

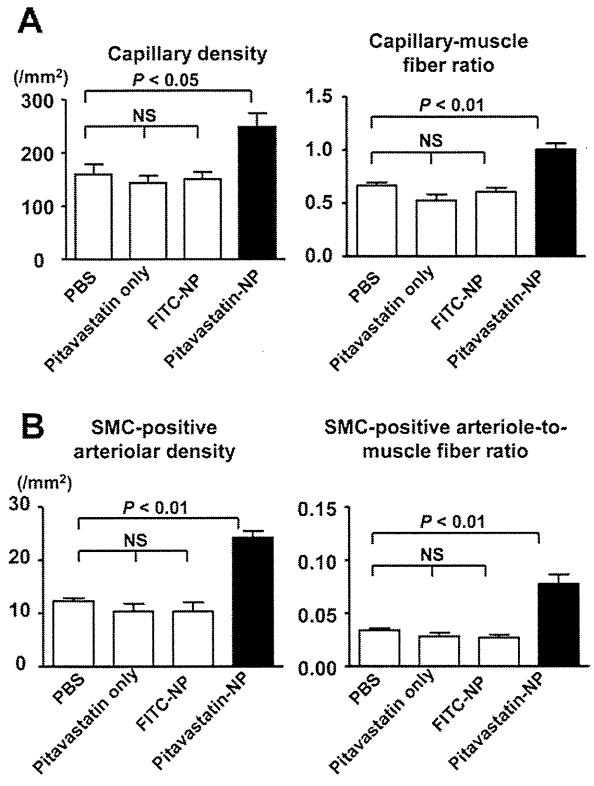

Fig 4. Effects of pitavastatin nanoparticles (*NP*) on angiogenesis and arteriogenesis are shown 28 days after treatment. **A,** CD-31$^+$ capillary density and capillary/muscle fiber ratio (indices of angiogenesis) is shown in ischemic muscles (n = 6 each). **B,** α-Smooth muscle actin (α-SMA)-positive arteriolar density and arteriole/muscle fiber ratio is shown in ischemic muscles (indices of arteriogenesis; n = 8 each). *FITC,* Fluorescein isothiocyanate; *PBS,* phosphate-buffered saline; *SMC,* smooth muscle cells.

nantly to capillaries and arterioles (Fig 5, *A*). Immunofluorescent staining revealed that FITC signals localized mainly to CD31$^+$ endothelial cells in FITC-NP–injected ischemic muscle 28 days after ischemia (Fig 5, *B*). In contrast, no FITC signals were observed in skeletal muscle myocytes on day 7 and 28 or in contralateral nonischemic hind limbs or remote organs (liver, spleen, kidney, and heart) at any time point (data not shown).

Effects of pitavastatin-NP on exercise-induced ischemia induced by electrical stimulation. To assess the functional efficacy of pitavastatin-NP on collateral arterial development, the effects of pitavastatin-NP on exercise-induced ischemia by electrical stimulation were examined. In the control PBS group, venous oxygen saturation in ischemic muscle decreased, and thus the difference in arteriovenous oxygen saturation increased after 15 and 30 minutes of electrical stimulation (Fig 6, *A*), suggesting the occurrence of exercise-induced ischemia. Treatment with pitavastatin-NP, but not with FITC-NP or pitavastatin only, abrogated the increase in arteriovenous oxygen difference in the ischemic limb (Fig 6, *B*). There were no significant differences in systemic blood hemoglobin levels among the four groups (data not shown).

Effects of vatalanib-NP on angiogenesis and arteriogenesis induced by pitavastatin-NP. We recently reported in a murine model that therapeutic neovascularization induced by pitavastatin-NP was mediated by increased eNOS activity and multiple endogenous angiogenic growth factors, such as VEGF.[10,25] Consequently, we examined VEGF expression in the four groups 28 days after treatment by immunohistochemistry and found increased VEGF positivity in CD31$^+$ endothelial cells of the capillaries and arterioles in the pitavastatin-NP group compared with other groups (Appendix Fig III, online only). Interestingly, positive VEGF staining was also detected in myocytes in the pitavastatin-NP group.

Vatalanib was selected because this molecule inhibits receptor tyrosine kinases of VEGR receptor types 1-3. Treatment with vatalanib-NP elicited no effects on angiographically visible collateral arterial development induced by hind limb ischemia in animals treated with PBS; however, it abrogated the arteriogenic response induced by pitavastatin-NP (Fig 7, *A* and *B*). In addition, treatment with vatalanib-NP abrogated histopathologic, angiogenic (capillary density), and arteriogenic (arteriolar density) responses induced by pitavastatin-NP (Fig 7, *C*). Vatalanib-NP elicited significant effects on histopathologic arteriogenic (arteriolar density) responses under baseline conditions (Fig 7, *C*).

Effects of pitavastatin-NP on angiogenesis and arteriogenesis in flt-1 TK$^{-/-}$ mice transfected with and without the *sFlt-1* gene. To examine the role of VEGF receptors (flk-1 and flt-1), the effects of pitavastatin-NP on ischemia-induced neovascularization were examined in wild-type and flt-1 TK$^{-/-}$ mice (Appendix Fig IV, online only). Compared with wild-type mice, the therapeutic effects of pitavastatin-NP decreased but were still observed in flt-1 TK$^{-/-}$ mice. To further examine the role of flk-1, *sFlt-1* gene transfer was performed into flt-1 TK$^{-/-}$ mice. The *sFlt-1* gene transfer blunted the therapeutic effects of pitavastatin-NP.

DISCUSSION

The present study demonstrates that NP-mediated endothelial cell-selective delivery of pitavastatin increased the development of collateral arteries (arteriogenesis) and improved exercise-induced ischemia in a rabbit model of chronic hind limb ischemia, indicating that this novel cell-selective delivery system is feasible for therapeutic arteriogenesis. We selected this rabbit model for translation to clinical settings in humans because it represents a preclinical model of arteriogenesis after femoral artery occlusion,[26] as observed in patients with severe peripheral artery disease.

Stimulation of the growth of collateral arteries (arteriogenesis) is evolving as a new therapeutic option for patients with atherosclerotic occlusive vascular disease, even though induction of additional angiogenesis or vasculogenesis is beneficial.[11,13] We assumed that the vascular endothelium would be an appropriate cellular target for the development

Table. Serum biochemical profiles

Variable[a]	*PBS*	*FITC-NP*	*Pitavastatin only*	*Pitavastatin-NP*
CPK (U/L)				
Day 7	345 ± 30	766 ± 270	445 ± 98	385 ± 44
Day 14	279 ± 8	486 ± 38	459 ± 118	296 ± 18
Day 21	242 ± 16	535 ± 58	396 ± 72	252 ± 12
Day 28	275 ± 60	229 ± 15	275 ± 33	259 ± 31
AST (IU/L)				
Day 7	10 ± 1	19 ± 3	16 ± 2	10 ± 1
Day 14	7 ± 0.3	19 ± 3	19 ± 6	8 ± 3
Day 21	15 ± 1	20 ± 2	22 ± 7	19 ± 4
Day 28	31 ± 11	29 ± 6	18 ± 2	20 ± 2
ALT (IU/L)				
Day 7	36 ± 9	36 ± 10	38 ± 5	29 ± 11
Day 14	26 ± 1	34 ± 6	37 ± 7	33 ± 9
Day 21	38 ± 7	33 ± 5	37 ± 8	43 ± 11
Day 28	42 ± 8	41 ± 10	35 ± 11	53 ± 19
BUN (mg/dl)				
Day 7	24 ± 0.2	17.3 ± 0.2	18 ± 1.5	24 ± 2
Day 14	23 ± 1	19.6 ± 2	24 ± 2	25 ± 1
Day 21	19 ± 1	18 ± 4	20 ± 2	19 ± 0.4
Day 28	26 ± 1	17 ± 0.3	17 ± 0.4	29 ± 2
Creatinine (mg/dL)				
Day 7	0.66 ± 0.01	0.82 ± 0.07	0.89 ± 0.01	0.80 ± 0.11
Day 14	0.70 ± 0.04	0.81 ± 0.09	0.87 ± 0.08	0.73 ± 0.05
Day 21	0.95 ± 0.02	0.80 ± 0.06	0.95 ± 0.01	1.03 ± 0.02
Day 28	0.85 ± 0.08	0.91 ± 0.06	0.86 ± 0.03	0.92 ± 0.03
Total cholesterol (mg/dL)				
Day 7	31 ± 10	31 ± 1	19 ± 5	46 ± 5
Day 14	26 ± 8	24 ± 3	19 ± 1	31 ± 4
Day 21	29 ± 10	18 ± 1	18 ± 3	32 ± 6
Day 28	18 ± 3	18 ± 2	21 ± 1	17 ± 2

ALT, Alanine aminotransferase; *AST,* aspartate transaminase; *BUN,* blood urea nitrogen; *CPK,* creatinine phosphokinase.
[a]Data are mean ± standard error of the mean (n = 3 each).

of collateral arteries after arterial occlusion because the endothelium plays a central role in the mechanism of arteriogenesis by expressing multiple growth factors and by recruiting monocytes and smooth muscle cells. We found that FITC signals were localized mainly to the vascular endothelium for up to 4 weeks after the injection of FITC-NP into ischemic skeletal muscles of rabbits in vivo, indicating that this NP-mediated delivery system may be useful as an innovative strategy for a therapy targeting endothelial cells. We recently reported that after cellular delivery of NP by endocytosis into endothelial cells, the PLGA NP escapes from the endosomal compartment to the cytoplasmic compartment and is retained in the cytoplasm, where release of the encapsulated drug occurs slowly in conjunction with the hydrolysis of PLGA.[10,27-29]

Daily administration of statins at high doses has been reported to augment arteriogenesis in normocholesterolemic rabbits.[6] These pleiotropic effects of statins are mediated through reduced levels of cholesterol biosynthesis pathway intermediates that serve as lipid attachments for post-translational modification (isoprenylation) of proteins, including Rho and Rac. Pitavastatin was selected as the NP compound because (1) pitavastatin elicited the most potent effects on the angiogenic activity of HECs in vitro compared with other statins, and (2) NP-mediated intracellular delivery of pitavastatin showed greater angiogenic activity of HECs compared with pitavastatin alone (Figs 1 and 2).

We also found in an in vivo rabbit model that (1) a single intramuscular injection of pitavastatin-NP increased the angiographic score in a dose-dependent manner, (2) pitavastatin (0.5 mg/kg) -NP significantly increased arteriogenesis and tissue oxygen pressure (tissue perfusion), and (3) the treatment of pitavastatin-NP increased immunoreactive VEGF expression selectively in vascular endothelial cells in the ischemic limb. Therefore, it is likely that that after NP-mediated endothelial delivery, pitavastatin is slowly released from the NP into the cytoplasm, resulting in significant therapeutic effects. Sata et al[8] reported that systemic daily administration of pitavastatin (1 mg/kg/day × 49 days = 49 mg/kg) has significant therapeutic effects in mice with hind limb ischemia. In our previous study, we reported the efficacy of pitavastatin (0.4 mg/kg)-NP in a murine model.[10] Therefore, at an approximately 100-fold lower dose, our NP-mediated delivery system is as effective as the cumulative systemic dose.

In clinical trials that examined the effects of a single vascular growth factor on peripheral and coronary artery disease, clinical end points such as increased exercise tolerance were negative or disappointing, although increased vascularity was noted.[14,15] It has been reported that limb hemodynamics, such as ankle-brachial index or muscle

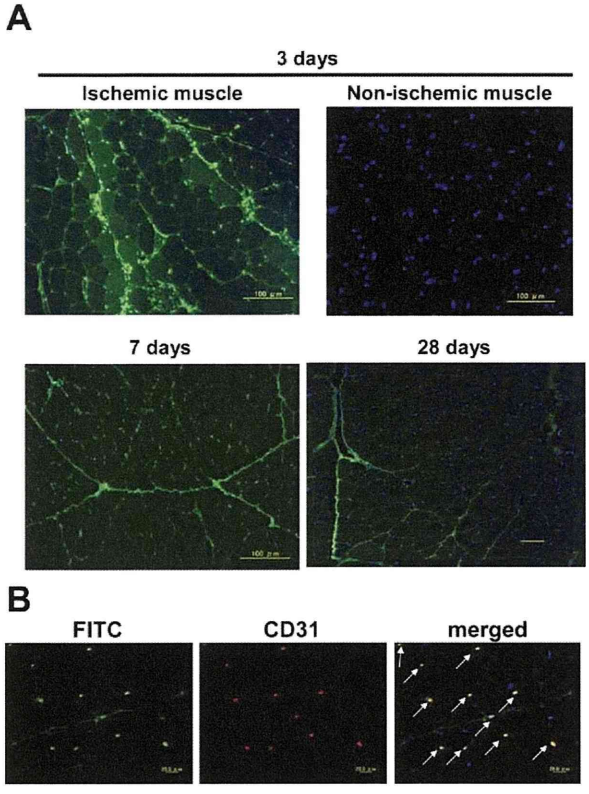

Fig 5. Cellular distribution of nanoparticles is shown in ischemic muscles. **A,** Fluorescent photomicrographs show cross sections of control nonischemic muscle and ischemic muscles at 3, 7, and 28 days after fluorescein isothiocyanate *(FITC)* nanoparticle *(NP)* injection. Nuclei were counterstained with 4′,6-diamidino-2-phenylindole *(blue)*. Fluorescence microscopic settings (exposure, filter, excitation light intensity, etc.) were the same for all images. Scale bar = 100 μm. **B,** Photomicrographs of cross sections of ischemic muscle 28 days after FITC-NP injection stained immunohistochemically with the endothelial marker CD31 *(red)*. Most FITC signals colocalized with the vascular endothelium *(arrows)*. Scale bars = 20 μm.

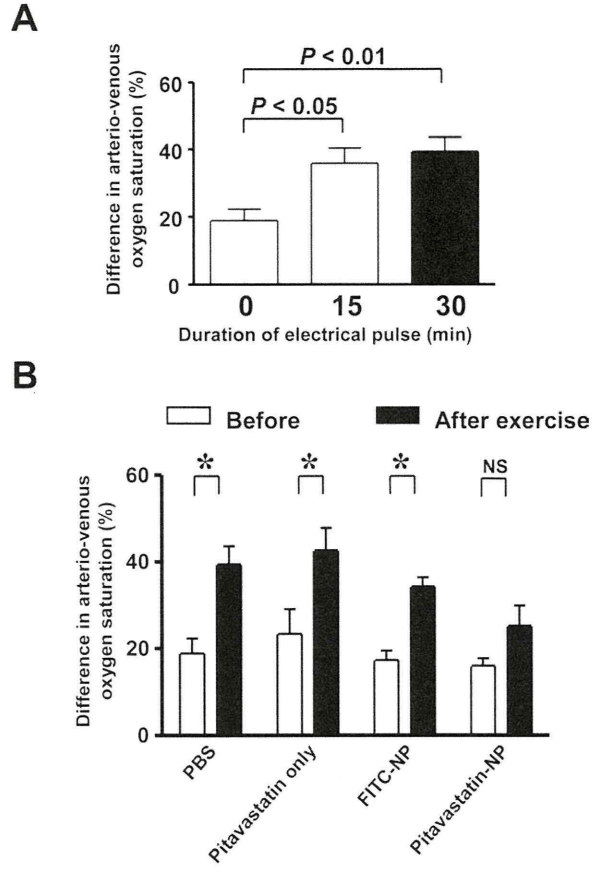

Fig 6. Effects are shown of pitavastatin nanoparticles *(NP)* on exercise-induced ischemia induced by electrical stimulation. **A,** Oxygen saturation in the femoral artery and vein in ischemic muscle is shown before and 15 and 30 minutes after muscular exercise by electrical stimulation in the phosphate-buffered saline *(PBS)* group (n = 6 each). **B,** The difference in arterial and venous oxygen saturation after 30 minutes of electrical pulse is shown in the four groups (n = 6 each). *FITC,* Fluorescein isothiocyanate.

blood flow at rest, are not correlated with functional capacity (claudication time or walking distance) in patients with peripheral arterial disease.[30] Therefore, assessment of the functional capacity of neovessels is needed in preclinical studies in animals. In other words, the improved functional capacity of collateral arteries must be a clinically important therapeutic goal in preclinical studies; however, few previous preclinical studies have addressed this point.

In the present study, we demonstrate that the arteriovenous oxygen difference in the ischemic hind limb increased in response to exercise in the PBS group, suggesting the development of exercised-induced ischemia. Treatment with pitavastatin-NP, but not with FITC-NP or pitavastatin only, prevented the development of exercise-induced ischemia. These data suggest that therapeutic arteriogenesis induced by pitavastatin-NP is associated with improved functional capacity.

We previously reported that the beneficial therapeutic effects induced by pitavastatin-NP are mediated by increased eNOS activity and multiple endogenous angiogenic growth factors in a murine model.[10] Recent reports by others have shown that mice lacking VEGF receptor 1 or placenta growth factor (a specific agonist of VEGR receptor 1), but not those lacking VEGF receptor 2, display impaired development of ischemia-induced angiogenesis and arteriogenesis.[31-33] However, roles of endogenous angiogenic growth factors in the mechanism of therapeutic effects of pitavastatin-NP have not been addressed.

In the present study, vatalanib-NP abrogated arteriogenic and angiogenic responses to pitavastatin-NP in rabbits. Furthermore, experiments with flt-1 $TK^{-/-}$ mice transfected with or without the *sFlt-1* gene showed partial contribution of both flt-1 and flk-1 to therapeutic angiogenic effects of pitavastatin-NP. These findings suggest that pitavastatin-NP produces an integrative system to form

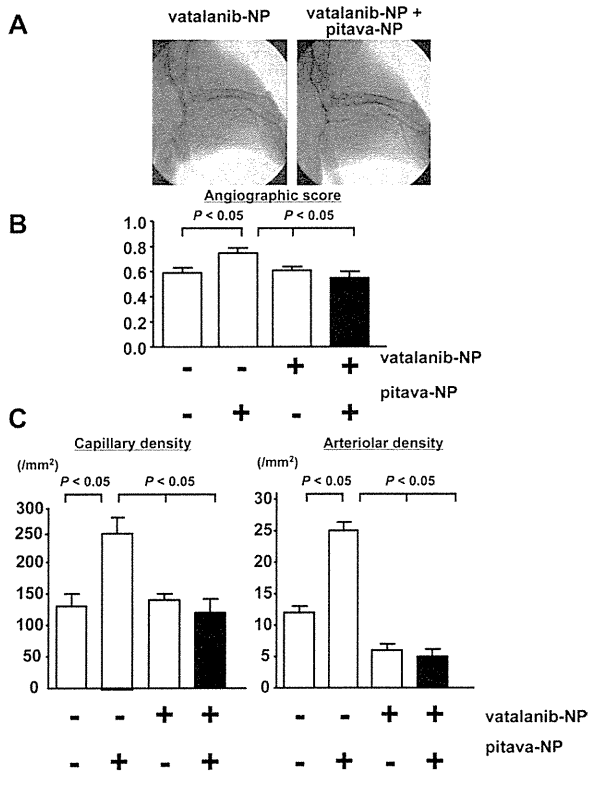

Fig 7. Effects of vatalanib nanoparticles *(NP)* are shown on angiogenesis and arteriogenesis induced by pitavastatin-NP. **A,** Representative angiograms show vatalanib-NP only and vatalanib-NP plus pitavastatin-NP groups 28 days after treatment. **B,** Summary of the angiographic scores obtained for the four groups (n = 3 each). **C,** Effects of vatalanib-NP are shown on histopathologic angiographic (capillary density) and arteriogenic (SMC-positive arteriolar density) responses induced by pitavastatin-NP.

functionally mature collaterals by controlled expression of endogenous VEGF and its receptor signals.

There are several limitations to the present study. First, only a single intramuscular injection of pitavastatin-NP was examined. In clinical settings, repetitive administration of an optimal dose may produce greater therapeutic effects. Second, we did not examine the contribution of bone marrow-derived progenitor cells because appropriate antibodies for detecting endothelial or smooth muscle progenitor cells are not available in rabbits. Further studies are needed to examine whether therapeutic effects afforded by pitavastatin-NP are associated with an increase in circulating endothelial progenitor cells.

CONCLUSIONS

This nanotechnology platform for vascular endothelial cell-selective delivery of pitavastatin is a promising strategy for the treatment of patients with severe organ ischemia and represents a significant advance in therapeutic arteriogenesis over current approaches. The nanotechnology platform may be further developed as a more effective and safer approach for therapeutic neovascularization.

AUTHOR CONTRIBUTIONS

Conception and design: SO, KE
Analysis and interpretation: SO, RN, KN, KE
Data collection: SO, RN, KN, KE
Writing the article: SO, KN, TM, KE
Critical revision of the article: SO, RN, KN, KE
Final approval of the article: SO, RN, KN, TM, MK, KS, RT, KE
Statistical analysis: SO, KN, KE
Obtained funding: KE
Overall responsibility: SO, KE

REFERENCES

1. Takemoto M, Liao JK. Pleotropic effects of 3-hydroxy-3-methylglutaryl coenzyme a reductase inhibitors. Arterioscler Thromb Vasc Biol 2001; 21:1712-9.
2. Egashira K, Hirooka Y, Kai H, Sugimachi M, Suzuki S, Inou T, et al. Reduction in serum cholesterol with pravastatin improves endothelium-dependent coronary vasomotion in patients with hypercholesterolemia. Circulation 1994;89:2519-24.
3. Ni W, Egashira K, Kataoka C, Kitamoto S, Koyanagi M, Inoue S, et al. Antiinflammatory and antiarteriosclerotic actions of HMG-CoA reductase inhibitors in a rat model of chronic inhibition of nitric oxide synthesis. Circ Res 2001;89:415-21.
4. Dimmeler S, Aicher A, Vasa M, Mildner-Rihm C, Adler K, Tiemann M, et al. HMG-CoA reductase inhibitors (statins) increase endothelial progenitor cells via the PI 3-kinase/Akt pathway. J Clin Invest 2001; 108:391-7.
5. Llevadot J, Murasawa S, Kureishi Y, Uchida S, Masuda H, Kawamoto A, et al. HMG-CoA reductase inhibitor mobilizes bone marrow—derived endothelial progenitor cells. J Clin Invest 2001;108:399-405.
6. Kureishi Y, Luo Z, Shiojima I, Bialik A, Fulton D, Lefer DJ, et al. The HMG-CoA reductase inhibitor simvastatin activates the protein kinase Akt and promotes angiogenesis in normocholesterolemic animals. Nat Med 2000;6:1004-10.
7. Kitamoto S, Nakano K, Hirouchi Y, Kohjimoto Y, Kitajima S, Usui M, et al. Cholesterol-lowering independent regression and stabilization of atherosclerotic lesions by pravastatin and by antimonocyte chemoattractant protein-1 therapy in nonhuman primates. Arterioscler Thromb Vasc Biol 2004;24:1522-8.
8. Sata M, Nishimatsu H, Osuga J, Tanaka K, Ishizaka N, Ishibashi S, et al. Statins augment collateral growth in response to ischemia but they do not promote cancer and atherosclerosis. Hypertension 2004;43:1214-20.
9. Zbinden S, Brunner N, Wustmann K, Billinger M, Meier B, Seiler C. Effect of statin treatment on coronary collateral flow in patients with coronary artery disease. Heart 2004;90:448-9.
10. Kubo M, Egashira K, Inoue T, Koga J, Oda S, Chen L, et al. Therapeutic neovascularization by nanotechnology-mediated cell-selective delivery of pitavastatin into the vascular endothelium. Arterioscler Thromb Vasc Biol 2009;29:796-801.
11. Schaper W, Scholz D. Factors regulating arteriogenesis. Arterioscler Thromb Vasc Biol 2003;23:1143-51.
12. Isner JM. Myocardial gene therapy. Nature 2002;415:234-9.
13. Heil M, Schaper W. Influence of mechanical, cellular, and molecular factors on collateral artery growth (arteriogenesis). Circ Res 2004;95: 449-58.
14. Losordo DW, Dimmeler S. Therapeutic angiogenesis and vasculogenesis for ischemic disease. Part I: angiogenic cytokines. Circulation 2004;109:2487-91.
15. Losordo DW, Dimmeler S. Therapeutic angiogenesis and vasculogenesis for ischemic disease: part II: cell-based therapies. Circulation 2004; 109:2692-7.
16. Ohtani K, Egashira K, Hiasa K, Zhao Q, Kitamoto S, Ishibashi M, et al. Blockade of vascular endothelial growth factor suppresses experimental restenosis after intraluminal injury by inhibiting recruitment of monocyte lineage cells. Circulation 2004;110:2444-52.

17. Zhao Q, Egashira K, Hiasa K, Ishibashi M, Inoue S, Ohtani K, et al. Essential role of vascular endothelial growth factor and Flt-1 signals in neointimal formation after periadventitial injury. Arterioscler Thromb Vasc Biol 2004;24:2284-9.
18. Zhao Q, Ishibashi M, Hiasa K, Tan C, Takeshita A, Egashira K. Essential role of vascular endothelial growth factor in angiotensin II-induced vascular inflammation and remodeling. Hypertension 2004;44:264-70.
19. Carmeliet P, Jain RK. Angiogenesis in cancer and other diseases. Nature 2000;407:249-57.
20. Wood JM, Bold G, Buchdunger E, Cozens R, Ferrari S, Frei J, et al. PTK787/ZK 222584, a novel and potent inhibitor of vascular endothelial growth factor receptor tyrosine kinases, impairs vascular endothelial growth factor-induced responses and tumor growth after oral administration. Cancer Res 2000;60:2178-89.
21. Kobayashi K, Kondo T, Inoue N, Aoki M, Mizuno M, Komori K, et al. Combination of in vivo angiopoietin-1 gene transfer and autologous bone marrow cell implantation for functional therapeutic angiogenesis. Arterioscler Thromb Vasc Biol 2006;26:1465-72.
22. Takeshita S, Zheng LP, Brogi E, Kearney M, Pu LQ, Bunting S, et al. Therapeutic angiogenesis. A single intraarterial bolus of vascular endothelial growth factor augments revascularization in a rabbit ischemic hind limb model. J Clin Invest 1994;93:662-70.
23. Babu AN, Murakawa T, Thurman JM, Miller EJ, Henson PM, Zamora MR, et al. Microvascular destruction identifies murine allografts that cannot be rescued from airway fibrosis. J Clin Invest 2007;117:3774-85.
24. Koga J, Matoba T, Egashira K, Kubo M, Miyagawa M, Iwata E, et al. Soluble Flt-1 gene transfer ameliorates neointima formation after wire injury in flt-1 tyrosine kinase-deficient mice. Arterioscler Thromb Vasc Biol 2009;29:458-64.
25. Hiasa K, Ishibashi M, Ohtani K, Inoue S, Zhao Q, Kitamoto S, et al. Gene transfer of stromal cell-derived factor-1alpha enhances ischemic vasculogenesis and angiogenesis via vascular endothelial growth factor/endothelial nitric oxide synthase-related pathway: next-generation chemokine therapy for therapeutic neovascularization. Circulation 2004; 109:2454-61.
26. Hoefer IE, van Royen N, Buschmann IR, Piek JJ, Schaper W. Time course of arteriogenesis following femoral artery occlusion in the rabbit. Cardiovasc Res 2001;49:609-17.
27. Nakano K, Egashira K, Masuda S, Funakoshi K, Zhao G, Kimura S, et al. Formulation of nanoparticle-eluting stents by a cationic electrodeposition coating technology efficient nano-drug delivery via bioabsorbable polymeric nanoparticle-eluting stents in porcine coronary arteries. JACC Cardiovasc Interv 2009;2:277-83.
28. Kimura S, Egashira K, Nakano K, Iwata E, Miyagawa M, Tsujimoto H, et al. Local delivery of imatinib mesylate (STI571)-incorporated nanoparticle ex vivo suppresses vein graft neointima formation. Circulation 2008;118:S65-70.
29. Kimura S, Egashira K, Chen L, Nakano K, Iwata E, Miyagawa M, Tsujimoto H, et al. Nanoparticle-mediated delivery of nuclear factor kappaB decoy into lungs ameliorates monocrotaline-induced pulmonary arterial hypertension. Hypertension 2009;53:877-83.
30. Hiatt WR, Regensteiner JG, Hargarten ME, Wolfel EE, Brass EP. Benefit of exercise conditioning for patients with peripheral arterial disease. Circulation 1990;81:602-9.
31. Clayton JA, Chalothorn D, Faber JE. Vascular endothelial growth factor-A specifies formation of native collaterals and regulates collateral growth in ischemia. Circ Res 2008;103:1027-36.
32. Pipp F, Heil M, Issbrucker K, Ziegelhoeffer T, Martin S, van den Heuvel J, et al. VEGFR-1-selective VEGF homologue PlGF is arteriogenic: evidence for a monocyte-mediated mechanism. Circ Res 2003; 92:378-85.
33. Nishi J, Minamino T, Miyauchi H, Nojima A, Tateno K, Okada S, et al. Vascular endothelial growth factor receptor-1 regulates postnatal angiogenesis through inhibition of the excessive activation of Akt. Circ Res 2008;103:261-8.

Submitted Aug 19, 2009; accepted Mar 10, 2010.

Additional online materials and results for this article may be found online at www.jvascsurg.org.

Circulation Journal
Official Journal of the Japanese Circulation Society
http://www.j-circ.or.jp

REVIEW

Oxidative Stress and Central Cardiovascular Regulation

– Pathogenesis of Hypertension and Therapeutic Aspects –

Yoshitaka Hirooka, MD; Yoji Sagara, MD; Takuya Kishi, MD; Kenji Sunagawa, MD

Oxidative stress is a key factor in the pathogenesis of hypertension and target organ damage, beginning in the earliest stages. Extensive evidence indicates that the pivotal role of oxidative stress in the pathogenesis of hypertension is due to its effects on the vasculature in relation to the development of atherosclerotic processes. It remains unclear, however, whether oxidative stress in the brain, particularly the autonomic nuclei (including the vasomotor center), has an important role in the occurrence and maintenance of hypertension via activation of the sympathetic nervous system. The aim of the present review is to describe the contribution of oxidative stress in the brain to the neural mechanisms that underlie hypertension, and discuss evidence that brain oxidative stress is a potential therapeutic target. (*Circ J* 2010; **74:** 827–835)

Key Words: Blood pressure; Brain; Heart rate; Hypertension; Sympathetic nervous system

Accumulating evidence indicates that the sympathetic nervous system plays an important role in the pathogenesis of hypertension.[1–3] Activation of the sympathetic nervous system is involved in the stages, clinical forms, 24-h blood pressure patterns, end-organ damage, and metabolic abnormalities of hypertension.[1–3] Although peripheral factors are also involved, the central nervous system (CNS) mechanisms are considered crucial.[3–7] The results of recent studies strongly suggest that central sympathetic outflow is increased in hypertension.[3–7] Increased oxidative stress is also involved in the pathogenesis of hypertension.[8] Although there have been many studies regarding target organ damage in hypertension, relatively few studies have addressed the role of oxidative stress in sympathetic nervous system activation.[9–11] Based on the role of angiotensin II (Ang II) in the generation of reactive oxygen species (ROS), the relationship between brain angiotensin and central sympathetic outflow has been examined.[12,13] Our group was the first to report that increased ROS generation in the brainstem contributes to the neural mechanisms of hypertension in hypertensive rats,[14] and we and other investigators have reported additional evidence to support this concept and the potential therapeutic aspects.[9–11] This review focuses on the role of oxidative stress within the brain in the neural pathogenesis of hypertension.

Increased Oxidative Stress in the Brain in Hypertension

Among the target organs of hypertensive vascular diseases, the brain is most affected by aging and oxidative stress.[15,16] Cell membranes in the brain contain a high concentration of polyunsaturated fatty acids. These fatty acids are targeted by ROS, which elicit chain reactions of lipid peroxidation. Oxidative stress is determined by measuring levels of thiobarbituric acid-reactive substances (TBARS), end products of lipid peroxidation. The levels of TBARS reflect those of malondialedehyde, although the assay is not specific for malondialedehyde.[15,17] There are some important points, however, for assessing the levels of TBARS.[17] The medium used for tissue preparation needs to contain a chelating agent and an antioxidant, and conditions for the assay must be kept constant. Therefore, we used another method for assessing the ROS production, which is electron spin resonance (ESR) spectroscopy. The amount of ROS was quantified by monitoring the time-dependent decay of the amplitude of the ESR spectra produced by the nitroxide radical 4-hydroxy-2,2,6,6-tetramethyl-piperidine-*N*-oxyl (hydroxyl-TEMPO) as a spin probe.[9,14] The signal decay of ESR spectroscopy reflects oxidative stress more directly. Also, it has an advantage for in vivo study.[18] We evaluated oxidative stress in the brains of stroke-prone spontaneously hypertensive rats (SHRSP) compared with normotensive Wistar–Kyoto (WKY) rats.[9,14] The rostral ventrolateral medulla (RVLM) is the major vasomotor center that determines basal sympathetic nervous system activity and it is essential for the maintenance of basal vasomotor tone.[3–7] Spontaneously hypertensive rats (SHR) or SHRSP exhibit increased sympathetic nervous system activity during the development of hypertension and are commonly used in experimental studies as models of human essential hypertension.[3–7] We previously investigated whether ROS are increased in the RVLM of SHRSP.[14] First, we found that ROS levels measured by TBARS and ESR spectroscopy were increased in the RVLM of SHRSP compared with WKY

Received February 19, 2010; revised manuscript received March 25, 2010; accepted March 26, 2010; released online April 15, 2010
Department of Cardiovascular Medicine, Kyushu University Graduate School of Medical Sciences, Fukuoka, Japan
Mailing address: Yoshitaka Hirooka, MD, Department of Cardiovascular Medicine, Kyushu University Graduate School of Medical Sciences, 3-1-1 Maidashi, Higashi-ku, Fukuoka 812-8582, Japan. E-mail: hyoshi@cardiol.med.kyushu-u.ac.jp
ISSN-1346-9843 doi:10.1253/circj.CJ-10-0153

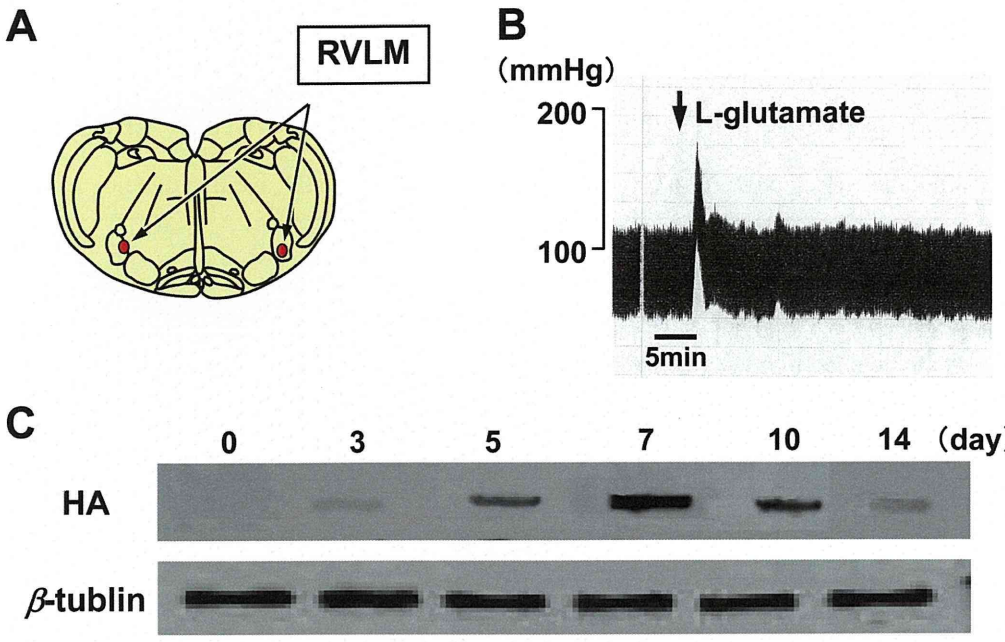

Figure 1. In vivo gene transfer of dominant-negative Rac1 into the rostral ventrolateral medulla (RVLM). (**A**) Schematic diagram showing the transfection sites. Gene transfer of adenovirus encoding dominant negative Rac1 (AdDNRac1) bilaterally into the RVLM (1.4×10^9 pfu/ml; 500 nl/site). (**B**) Transfection sites were confirmed by prior microinjection of L-glutamate. (**C**) Time course of AdDNRac1 expression levels in the RVLM on western blot. HA, hemagglutinin.

rats. In addition, superoxide dismutase (SOD) expression and activity, which are ROS scavenging factors, were decreased in the RVLM of SHRSP compared with WKY rats. Functionally, microinjection of the membrane-permeable radical scavenger tempol into the RVLM decreased blood pressure, heart rate, and sympathetic nervous system activity in SHRSP but not in WKY rats. More importantly, overexpression of Mn-SOD, an antioxidant enzyme, in the RVLM of SHRSP decreased blood pressure and sympathetic nervous system activity. These findings strongly indicate that oxidative stress in the RVLM is increased in SHRSP and contributes to the neural mechanisms of hypertension. As described here, brain ROS is one of the results of generalized target organ damage, appearing earlier in the brain due to its susceptibility. The brain ROS would increase blood pressure via activation of the sympathetic nervous system and this would ultimately result in a vicious cycle. It would be possible, however, that brain ROS is involved in the early stage of hypertension in SHR or SHRSP, because we found that oxidative stress in the brain assessed on in vivo ESR was enhanced in young (6-week-old) SHR or SHRSP compared with age-matched WKY rats (unpublished data). The levels of TBARS were not different, probably because the levels of TBARS reflect lipid peroxidation caused by ROS. Other investigators also found that an increase in superoxide anions in the RVLM is associated with hypertension in SHR,[19] and reduced expression and activity in Cu/Zn-SOD and Mn-SOD within the RVLM contribute to oxidative stress and neurogenic hypertension in SHR.[20] An increase in oxidative stress within the RVLM also plays an important role in maintaining high arterial blood pressure and sympathetic activation in 2-kidney 1-clip (2K-1C) hypertensive rats, which is a renovascular hypertension model.[21] In that study, Oliveira-Sales et al demonstrated that the mRNA expression of NAD(P)H oxidase subunits ($p47^{phox}$ and $gp91^{phox}$) in the RVLM was greater in 2K-1C than in the control group. Interestingly, there were no differences in Cu/Zn-SOD expression between the two groups. TBARS levels in the RVLM were significantly greater in the 2K-1C than in the control group, suggesting enhanced oxidative stress. Functionally, microinjection of vitamin C into the RVLM decreased blood pressure and renal sympathetic nerve activity in 2K-1C but not in controls. Importantly, in a subsequent study, these authors suggested that the paraventricular nucleus of the hypothalamus is also involved.[22] Notably, although 2K-1C is a model of renovascular hypertension, suggesting that circulating Ang II is increased, angiotensin type I (AT1) receptor gene expression levels within the RVLM and paraventricular nucleus were upregulated in this model, indicating that ROS was produced via the activation of nicotinamide-adenine dinucleotide phosphate [NAD(P)H] oxidase.

Sources of ROS Production in the Brain

As a source of ROS production in the CNS, NAD(P)H oxidase is a major player. NAD(P)H oxidase is composed of two membrane-bound subunits, $gp91^{phox}$ and $p22^{phox}$; several cytoplasmic subunits, $p47^{phox}$, $p40^{phox}$, and $p67^{phox}$; and the small G-protein Rac1.[23–26] Stimulation of AT1 receptors activates NAD(P)H oxidase by which the cytoplasmic subunits of Rac1NAD(P)H oxidase such as Rac1 bind to the membrane subunits, thereby activating the enzyme leading to superoxide generation. Rac1 requires lipid modification to migrate from the cytosol to the plasma membrane, which is a necessary step for activating ROS-generating NAD(P)H oxidase. NAD(P)H oxidase activity is greater in the brainstem of SHRSP than in that of WKY.[27,28] We transfected adenovirus

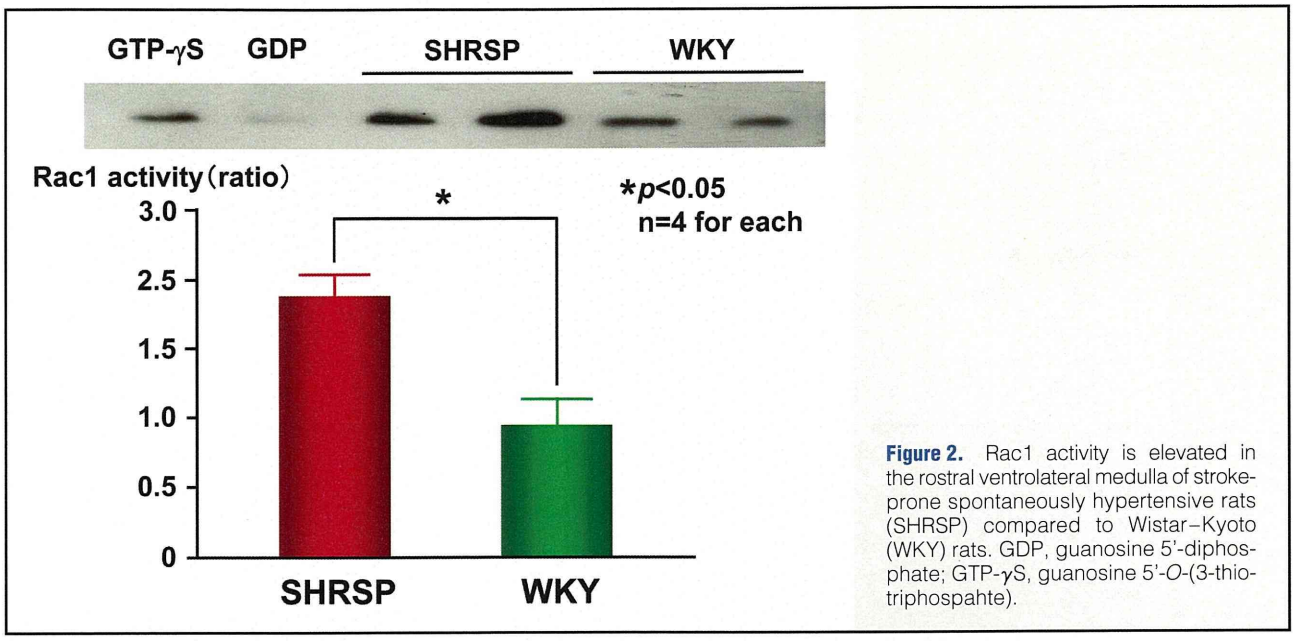

Figure 2. Rac1 activity is elevated in the rostral ventrolateral medulla of stroke-prone spontaneously hypertensive rats (SHRSP) compared to Wistar–Kyoto (WKY) rats. GDP, guanosine 5'-diphosphate; GTP-γS, guanosine 5'-*O*-(3-thiotriphospahte).

encoding dominant-negative Rac1 into the RVLM of SHRSP and WKY rats (Figure 1).[27] Rac1 activity in the RVLM tissue was increased in SHRSP compared to WKY rats (Figure 2).[27] Importantly, we demonstrated that inhibition of Rac1-derived ROS in the RVLM decreased blood pressure, heart rate, and urinary norepinephrine excretion in SHRSP (Figure 3).[27] A similar response occurs after inhibition of Rac1-derived ROS in the nucleus tractus solitarius (NTS).[28]

In addition to the cytosolic production of ROS, mitochondria are the primary source of ROS production in many cells. Ang II increases mitochondrial ROS production in the RVLM, leading to sympathoexcitation.[29] Furthermore, NAD(P)H oxidase-derived ROS might trigger Ca^{2+} accumulation, which leads to mitochondrial ROS production.[29] This suggestion is based on the finding that gene transfer of dominant negative Rac1 attenuated the Ang II-induced increase in reduced Mito-Tracker red fluorescence.[29] In contrast, impairment of mitochondrial electron transport chain complexes in the RVLM might be involved in the neural abnormality underlying hypertension in SHR.[30] This issue was recently discussed by Zimmerman and Zucker.[31] Although we did not detect impairment of brain mitochondrial respiratory complexes in SHRSP, we propose that mitochondria-derived ROS mediate sympathoexcitation via NAD(P)H oxidase activation.[29]

Another possibility for ROS generation is uncoupling nitric oxide synthase (NOS). In the absence of L-arginine or with tetrahydrobiopterin, NO production from inducible NOS (iNOS) causes uncoupling from the oxidation of NADPH, resulting in superoxide generation.[9] iNOS overexpression in the RVLM causes hypertension and sympathoexcitation that is mediated by an increase in oxidative stress.[32] This might be relevant to our observation that iNOS expression levels in the RVLM are greater in SHRSP than in WKY rats.[33] In addition, microinjection of iNOS antagonists into the RVLM reduces blood pressure only in SHR, but not in WKY rats.[33]

ROS-Mediated Activation of Transcriptional Factors

It has been suggested that an Ang II-mediated influx of Ca^{2+} in neurons depends on increased superoxide generation by a Rac1-dependent NAD(P)H oxidase.[34] Ang II also regulates neuronal activity via inhibition of the delayed rectifier potassium current.[35] Ang II-mediated upregulation of L-type Ca^{2+} currents in neurons isolated from the NTS is inhibited by scavenging ROS, indicating a role for NAD(P)H oxidase-derived superoxide in the activation of Ca^{2+} channels in the NTS.[24]

NAD(P)H oxidase-derived superoxide mediates an Ang II-induced pressor effect via the activation of p38 mitogen-activated protein kinase (MAPK) in the RVLM.[36] Recently, we suggested that AT1 receptor-activated caspase-3 acting through the Ras/p38 MAPK/extracellular signal-related protein kinase pathway in the RVLM is involved in sympathoexcitation in SHRSP.[37] These pathways may be downstream effectors of ROS in the RVLM, which in turn plays a crucial role in the pathogenesis of hypertension. Interestingly, the pro-apoptotic proteins Bax and Bad were enhanced and the anti-apoptotic protein Bcl-2 was decreased in the RVLM of SHRSP, and inhibition of caspase-3 normalized these changes in pro- and anti-apoptotic protein levels.[37] These alterations in the RVLM of SHRSP were stimulated by Ang II via activation of the AT1 receptors, which are upregulated in this strain and other hypertensive models.[38] It would be reasonable to consider that different mechanisms may be responsible for sympathoexcitation in different brain sites (influx of Ca^{2+} for RVLM, apoptosis for NTS), and activation of the apoptotic pathway is involved in sympathoexcitation in the RVLM.[37] The exact physiologic implication of these observations requires further evaluation.

Effects of Angiotensin Receptor Blockers on Brain Oxidative Stress

The existence of an independent renin–angiotensin system in the brain is well established. Activation of the brain renin–angiotensin system substantially contributes to the development and maintenance of hypertension through activation of the sympathetic nervous system, vasopressin release, and drinking behavior.[39,40] There is considerable evidence that

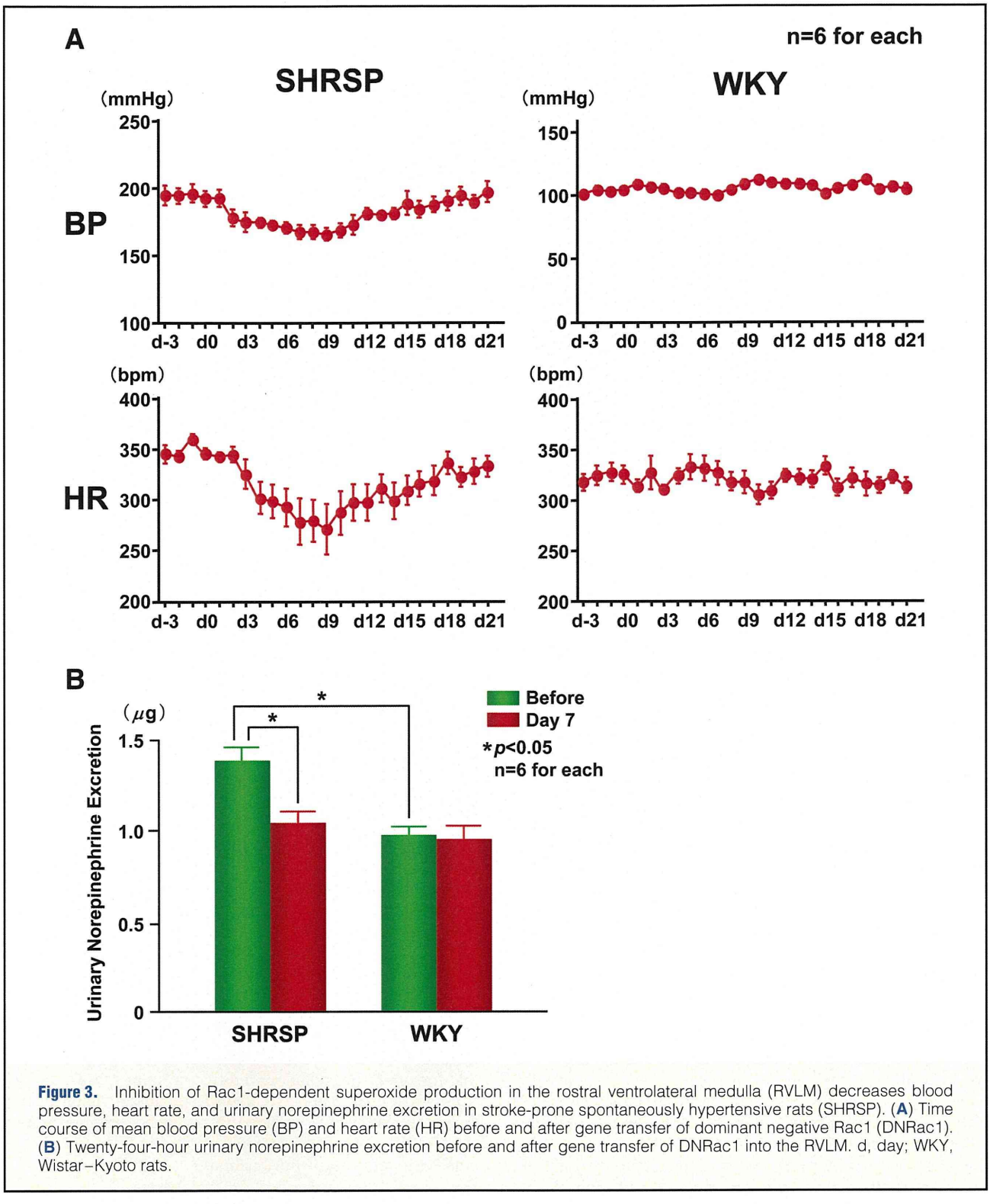

Figure 3. Inhibition of Rac1-dependent superoxide production in the rostral ventrolateral medulla (RVLM) decreases blood pressure, heart rate, and urinary norepinephrine excretion in stroke-prone spontaneously hypertensive rats (SHRSP). (**A**) Time course of mean blood pressure (BP) and heart rate (HR) before and after gene transfer of dominant negative Rac1 (DNRac1). (**B**) Twenty-four-hour urinary norepinephrine excretion before and after gene transfer of DNRac1 into the RVLM. d, day; WKY, Wistar–Kyoto rats.

peripherally administered angiotensin receptor blockers (ARBs) penetrate the blood–brain barrier, although there are some differences among ARBs.[41,42] AT1 receptors are abundant in the circumventricular organs, such as the subfornical organ and the organum vasculosum lamina terminalis, and the area postrema, which lack a blood–brain barrier.[39–42] Therefore, peripherally administered ARBs can also bind to those areas, thereby inhibiting the central actions of Ang II. Oral treatment with the ARB telmisartan appears to inhibit the central responses to Ang II in awake rats.[43] Although other ARBs also inhibit the central actions of Ang II within the brain beyond the blood–brain barrier,[41,42,44] these effects might differ depending on the pharmacokinetics and properties of each drug (ie, lipophilicity etc).[43] We evaluated the